FINAL REPORT ON

COUPLED THERMAL/SEEPAGE AND CONTAINMENT TRANSPORT MODELING FOR THE TAILINGS FACILITY MEADOWBANK GOLD PROJECT

Submitted to:

Agnico-Eagle Mines Limited
Meadowbank Division
Suite 375, 555 Burrard Street
Box 209, Two Bentall Centre
Vancouver, BC V7X 1M8

DISTRIBUTION:

3 Copies - Agnico-Eagle Mines Limited
2 Copies - Golder Associates Ltd.

07-1413-0074/6000
August 1, 2008 Doc. No. 722 Ver.0

Golder Associates Ltd.
500 - 4260 Still Creek Drive, Burnaby, British Columbia Canada V5C 6C6
Tel: (604) 296 4200 Fax: (604) 298 5253 www.golder.com

EXECUTIVE SUMMARY

Agnico Eagle Mines Ltd. (AEM) requested that Golder Associates Ltd. (Golder) undertake coupled seepage, thermal and contaminant transport analyses for the Tailings Storage Facility (TSF) as a design component of the Meadowbank Gold Project. The analyses are based on the previous modeling exercise done in 2007, but updated by coupling the thermal and seepage models, considering staged flooding of the Portage Pit, and adding a contaminant transport analysis which is semi-coupled with the seepage/thermal analysis. The modeling demonstrates that the proposed strategy for closure of the TSF is appropriate for minimizing water flux and contaminant transport from the TSF into Portage Lake. The model also indicates that the tailings will freeze and remain frozen for over 100 years after the mine closure irrespective of the impact of global warming.

The coupled seepage/thermal analysis shows that water flowing through the tailings will increase the time for the tailings to freeze completely. Nevertheless, the impact of heat transfer from water flow will be minimized by the expected low hydraulic conductivity of the tailings. In addition, the seepage component of the coupled analysis shows that water flux in the TSF will be mainly controlled in the short term by the hydraulic gradient existing between the tailings and the Portage Pit areas. Upon mine closure and flooding of the Portage Pit, the hydraulic gradient between the two areas will gradually reduce as the lake level rises and tailings drain. Hydrostatic equilibrium will occur within about 10 years causing flux from the tailings area to practically cease. After that, the freezing front will progressively advance into the tailings and the tailings will freeze within a period of about 40 years after closure.

A contaminant transport analysis was performed semi-coupled with the seepage/thermal analysis. The model assesses movement of contaminants driven by the diffusion and advection processes, and considers dilution of contaminant concentrations as the contaminant plume mixes with clean groundwater. The contaminant transport model assesses two different scenarios, with contaminant being transported during all times of mine operations, and with transport of contaminant occurring only after the end of deposition. In the first scenario, the model shows that contaminant loads would reach the Portage Pit area during the deposition phase. However, upon mine closure and flooding of the Portage Pit, water flux and consequent movement of contaminants by advection will stop associated with reduction in the hydraulic head and progressive freezing of the tailings. In addition, during flooding of the Portage Pit, clean water will infiltrate the ground and reduce the concentration of contaminants by dilution. In the second scenario, with contaminant transport occurring only after the end of deposition, the model indicates that contaminants will not reach the Portage Pit area, and the contaminant plume will be confined near the tailings foundation. In both scenarios, the model indicates that contaminant transport will not persist in the long term because of water flux restrictions.

Some of the design assumptions used in the seepage/thermal model are considered to be conservative, especially those associated with the evolution of tailings temperature during deposition. The complexity of the real time tailings heat exchange process could not be fully incorporated in the models, and a conservative approach was used in benefit of safety. In spite of the conservative approach used in some parts of the model, the model results still confirm that the main strategy to control contaminant transport from the TSF by encapsulating the tailings within the continuous permafrost zone is appropriate.

TABLE OF CONTENTS

SECTION PAGE
1.0 INTRODUCTION 1
2.0 UNDERSTANDING OF THE SYSTEM 2
3.0 MODEL ASSUMPTIONS AND LIMITATIONS 4
4.0 COUPLED SEEPAGE-THERMAL MODEL 5
4.1 Model Principles 5
4.2 Material Properties 5
4.2.1 Thermal Properties 5
4.2.2 Hydraulic Properties 11
4.3 Estimation of Ground Surface Temperature 11
4.3.1 Climate Data Review 11
4.3.2 Ground Temperature Estimation 13
4.3.3 Validation of the Ground Surface Temperature Function 14
4.4 Tailings Deposition Sequence 15
4.5 Models Configuration 18
4.5.1 Tailings Model 18
4.5.2 Tailings Storage Facility Model 20
5.0 CONTAMINANT TRANSPORT MODEL 23
6.0 MODEL RESULTS 24
6.1 Tailings Model 24
6.1.1 End of Deposition Temperatures for Different Scenarios 24
6.1.2 Evolution of Temperatures During Deposition 26
6.1.3 Influence of Water Flow 28
6.2 Tailings Storage Facility Model 30
6.2.1 Evolution of Temperatures 30
6.2.2 Evolution of Flow Rates 41
6.2.3 Sensitivity to Thawed Foundation During Deposition 51
7.0 CONCLUSIONS 53
8.0 REFERENCES 56

LIST OF TABLES

Table 1 Measured Thermal Conductivity of Tailings
Table 2 Material Properties Used in the Thermal Models
Table 3 Hydraulic Conductivity Values Used in the Models
Table 4 Tailings Deposition Sequence at Spigot 5 (Extracted from the Tailings Deposition Plan)
Table 5 Boundary Conditions Used in the Coupled Analysis
Table 6 Maximum Flow Rates Predicted Through the Central Dike

LIST OF FIGURES

Figure 1 Computed Depth of Freezing Front 10 Years After Operations Using the Tailings Thermal Conductivity Measured in the Laboratory and the Adjusted Values
Figure 2 Temperature Profile of Tailings Ten Years After Closure with Varying Volumetric Water Content
Figure 3 Air Temperature and Wind Speed Data
Figure 4 Total Precipitation and Relative Humidity
Figure 5 Calculated Ground Surface Temperature
Figure 6 General Ground Surface Temperature Function
Figure 7 Comparison Between Measured (M) and Computed (C) Temperature Profiles at Different Times (Reference Borehole 03gt-Td-1)
Figure 8 Warming and Cooling Cycles During Deposition for the Three Scenarios Considered
Figure 9 Example of Tailings Modeling Sequencing and Boundary Conditions Models Continued to Stage 15
Figure 10 1-D Tailings Model Sequencing with Tailings Elevation Increasing in 15 Stages
Figure 11 Computed Tailings Temperature at the End of Deposition for Scenario 1(Cooling Times Equal Inactive Times) with Different Tailings Deposition Temperatures
Figure 12 Computed Tailings Temperature at the End of Deposition for Scenario 2 (Cooling Times Equal 75% Inactive Times) With Different Tailings Deposition Temperatures
Figure 13 Computed Tailings Temperature at the End of Deposition for Scenario 3 (Cooling Times Equal 50% Inactive Times) With Different Tailings Deposition Temperatures
Figure 14 Computed Temperature Profiles of Tailings at Increasing Elevations at Different Times During the Deposition Phase
Figure 15 Evolution of Tailings Temperature with Time at Different Elevations of The Tailings Column
Figure 16 Computed Tailings Temperature Profiles at the End of Deposition With and Without Consideration to Water Flux
Figure 17 Computed Tailings Temperature Profiles 10 Years after Closure with and Without Consideration to Water Flux
Figure 18 Evolution of Tailings and Foundation Temperature for Winter (February) Times After the End of Deposition
Figure 19 Temperatures in the TSF at the end of Deposition (February 2013)
Figure 20 Temperatures in the TSF after Completion of the Portage Pit Flooding (February 2017)

Figure 21 Temperatures in the TSF 10 years after Closure (February 2023)
Figure 22 Temperatures in the TSF 20 years after Closure (February 2033)
Figure 23 Temperatures in the TSF 50 years after Closure (February 2053)
Figure 24 Temperatures in the TSF 100 years after Closure (February 2113)
Figure 25 Comparison of Tailings Temperature Profiles with Time for Depressing Freezing Points
Figure 26 Comparison of Unfrozen Water Content in the Tailings for Depressing Freezing Points
Figure 27 Evolution of Temperatures at the Top and Bottom of the Rock Cover in the Long Term
Figure 28 Evolution of Flow Rates through the Foundation with Time and Hydraulic Gradient between the Tailings and the Lake
Figure 29 Evolution of Flow Rates through the Foundation with time and Hydraulic Gradient between the Tailings and the Lake
Figure 30 Variation of the Water Table Location in the Tailings Storage Facility during flooding of the Portage Pit
Figure 31 Evolution of Flow Rates through the Portage Fault with Time and Hydraulic Gradient between the Tailings and the Lake
Figure 32 Evolution of Contaminant Loads from the Bottom of the Tailings after the Mine Closure
Figure 33 Evolution of Copper and Cyanide Loads from the Bottom of the Tailings after the Mine Closure
Figure 34 Concentration of Contaminants in the Foundation 1 Year after the Mine Closure
Figure 35 Concentration of Contaminants in the Foundation 2 Years after the Mine Closure
Figure 36 Concentration of Contaminants in the Foundation 5 Years after the Mine Closure
Figure 37 Evolution of Contaminants Loads during Deposition and after Closure Considering a Thawed Foundation
Figure 38 Normalized concentration of contaminants in the TST foundation after completion of the Portage Pit flooding considering a thawed foundation

1.0 INTRODUCTION

Seepage and thermal analyses were conducted separately in early 2007 as part of the design of the Central Dike for the Meadowbank Gold Project. It was later requested by Natural Resources Canada (NRCan) that thermal and seepage analyses be carried out together to evaluate the impact of water flow on the freezing process of the tailings. In addition, it was also requested that a contaminant transport model be developed to assess the potential migration of contaminants from the tailings area into the area of the Portage Pit, which is to be flooded upon mine closure.

The current analyses follow the same methodology described in the report "Detailed Design of Central Dike Meadowbank Gold Project" (Golder 2007b), but update the previous models by:

- Coupling thermal and seepage analyses during operations and post-closure;
- Considering staged flooding of the Portage Pit during a period of 4 years;
- Considering flooding and thawing of the rockfill within the dam body;
- Considering the impact of the Portage Fault on the seepage rates; and
- Conducting a contaminant transport analysis based on the flow velocities computed from the coupled seepage/thermal model.

Similarly to the modeling exercise carried out in 2007, the current model evaluates the evolution of tailings temperature during deposition using a sequential 1-D model based on the Tailings Deposition Plan. The Tailings Storage Facility (TSF) was then modeled through a 2-D model.

A global warming scenario was incorporated in the long term analysis.

2.0 UNDERSTANDING OF THE SYSTEM

Numerical models developed for large areas such as the TSF of the Meadowbank Gold Project are intended to assess the overall evolution of thermal, hydraulic and contaminant conditions of the site, but do not encompass all local variations that are certain to occur in the field. Therefore, initially it is important to identify such local variations and understand how their thermal, hydraulic and contaminant patterns would differ from the overall behavior predicted for the entire site. Tailings segregation during deposition, real-time instant heat exchange, cryoconcentration, and tailings drain down upon completion of deposition are some examples of dynamic processes that can result in localized changes in the thermal and hydraulic patterns. A brief description of these processes is presented below.

During low density slurry deposition particle segregation occurs on the beach with coarser particles settling near the spigot and finer particles being carried farther by the flow. The coarser material adjacent to the spigot drains and consolidates more rapidly then the fine tailings away from the spigot.

The segregation process within the Meadowbank TSF will affect the thermal and hydraulic behavior of the tailings adjacent to the dike. The coarse, segregated tailings will be denser than the average tailings and will have higher thermal conductivity values and lower volumetric water contents, which lead to a faster freezing process compared to the finer tailings located remote from the dike. Because the extent of the coarse materials near the dike is unknown at this point and will depend on the operation of the spigots and beach, the models assessed the overall freezing process of the average tailings, and sensitivity analyses are used to demonstrate how denser and dryer tailings would impact the local freezing process.

The temperature of tailings is constantly changing during deposition as tailings move away from the spigots, with heat flowing from the warm new tailings into the cold older tailings until a thermal equilibrium is attained. In addition, the temperature of newly deposited tailings is also affected by the air temperature at the time deposition occurs.

Based on this understanding of the dynamic process, the current study used an approach that accounted for warming and cooling cycles associated with active and inactive times in deposition sectors, and assessed the impact of different average tailings deposition temperatures and thermal properties on the final temperature profiles. The complex dynamic real-time heat exchange process that occurs during deposition can not be completely reproduced in a model and the computed results represent approximations of average temperature profiles and patterns.

Another factor that may play a role on the actual evolution of tailings temperature and the transport of contaminants is the process of cryoconcentration, which increases the concentration of solutes in the liquid phase due to solute exclusion ahead of the freezing front. One impact of this process is the progressive depression of the liquid phase freezing point as the solute concentration increases. This would cause water to remain in the liquid phase under sub-zero temperatures and therefore, sustain water flux and transport of substances in lower temperatures. A second impact is that the chemical gradient between the contaminant plume and uncontaminated areas would increase, causing the diffusion component of the transport of contaminant process to become more important.

The models developed in this study do not directly account for cryoconcentration, but examine the effect of overall freezing point depression comparing the temperature, unfrozen water content and flow rates through the tailings at freezing points of 0^{o}C and -2^{o}C. The models do not account for the progressive increase of contaminants concentration and gradual depression of the solution freezing point ahead of the freezing front.

Because of code limitations, the models also did not evaluate spatial variations that could result in high concentration solutions entrapped within frozen zones. This is likely to happen because the hydraulic conductivity of the tailings is expected to be low, and the freezing front may locally advance faster than solute is transported. Under this circumstance, lower concentration tailings portions with higher freezing point that are located below zones of high solute concentration could freeze and entrap the zones with higher concentration liquid solutions in ice.

Upon completion of deposition, the tailings near surface are expected to desaturate as the supply of process water ends. This will affect the thermal and hydraulic properties of the material and impact both the freezing and water flow processes, as well as the process of contaminant transport as flow velocities will decrease upon gradual reduction of the hydraulic gradient between the tailings and the Portage Pit areas. The models did account for this process and simulated the interaction between the tailings draindown and the staged flooding of the Portage Pit. However, the models did not evaluate the impact of snow melt and/rainfall in the rate of tailings desaturation. Depending on how much water infiltrates the tailings, the desaturation process could be slowed or even stopped, but separate detailed modeling would be necessary to evaluate this aspect. For the present study, it was considered that this additional model was not necessary because the Portage Pit flooding is the main component responsible for the reduction of the hydraulic gradient between the tailings and pit areas. Once the Portage Lake reaches its final elevation of 134.1 m, a near hydrostatic equilibrium condition will prevail between the TSF and the Portage Pit, with water/contaminant flow from the tailings area being markedly reduced.

3.0 MODEL ASSUMPTIONS AND LIMITATIONS

The present models use sequential and iterative analyses that together provide elements to understand the patterns of thermal, hydraulic and contaminant transport regimes that are expected to develop. The models are however simplifications of the field reality and several assumptions were made in terms of initial field conditions, material properties, and evolution of climate and ground temperatures. Most of the assumptions will be further discussed in this document, and other primary assumptions are as follows:

- The Tailings Storage Facility Area was assumed to be isolated from the adjacent lakes by permafrost. Therefore, flux from the tailings area was assumed to occur only toward the Portage Pit. Similarly, water flow into the tailings area was assumed to occur only from the Portage Pit upon flooding;

- Based on the Tailings Deposition Plan, tailings deposition is assumed to start in February. Therefore the foundation was assumed to be initially frozen to a depth of 3 m;

- Flooding of the Portage Pit at the end of operations and filling of the lake to its final elevation of 134.1 m is assumed to occur over a period of 4 years; and

- Global warming is considered to increase average air temperature of 6.4^{o}C over a period of 100 years (IPCC, 2007).

4.0 COUPLED SEEPAGE-THERMAL MODEL

4.1 Model Principles

The coupled seepage-thermal model was conducted by simultaneously using the codes TEMP/W and SEEP/W (v. 7.0.3) by Geoslope International Ltd.

In a coupled analysis, both the SEEP/W and TEMP/W solvers run at the same time and share information. When the analysis starts, SEEP/W computes and passes to TEMP/W the volumetric water content and the x, y velocities in the model geometry. TEMP/W uses this data to perform the convective heat transfer for flowing water, computes the new temperatures and passes the information back to SEEP/W, which uses the data when computing the different hydraulic conductivities of the materials under frozen and unfrozen conditions. If the ground starts to freeze, then the hydraulic conductivity starts to decrease based on the equivalent cryogenic suction that would be established for the range of temperatures below the phase change point. The iterating process continues over the time step until the solution converges at each time.

4.2 Material Properties

4.2.1 Thermal Properties

A portion of tailings was specifically generated for laboratory measurement of thermal conductivity under frozen and unfrozen conditions. The sample was prepared by crushing of individual ore samples from the three pits (Portage, Vault and Goose Island) to the grain size of the final tailings. The crushed ores were then proportionally combined (51% Portage, 39% Vault and 10% Goose Island) and slurried with a synthetic supernatant solution to mimic what is expected to be the actual tailings chemistry. The result of the thermal conductivity test is presented in Table 1.

TABLE 1: Measured Thermal Conductivity of Tailings

Sample Parameters	Thermal Conductivity (W/m ^{o}C)
Dry density = 1711 kg/m^3 Void ratio = 0.74 Gravimetric water content = 19.2% Saturation = 77.5 %	Unfrozen (T 16.4^{o}C) = 1.98 Frozen (T -18.0^{o}C) = 3.21

Within the TSF, the tailings are expected to have a lower average density and higher average water content than tested in the laboratory, and this will cause the thermal conductivity to be lower. The adjusted values are presented in Table 2.

The thermal conductivity of the other materials was primarily defined based on the Johansen equation (Johansen, 1975), as well as reported values from the literature (Geoslope 2004, Nidal H, 2000 and MEND 1998). The volumetric heat capacity of the materials was estimated based on the method proposed by Johnston et al. (1981). Table 2 presents the material properties and the estimated thermal properties that were considered in the analyses. Geotechnical properties for the foundation, dike and tailings materials were established based on current project data.

The bedrock at the site includes greenstone ultramafic and mafic flow sequences, metasedimentary and intermediate volcanics rocks. The tailings material is processed iron formation and intermediate volcanic rock.

Estimates of the unfrozen water content relationship with temperature were made for the tailings and foundation materials using the relationship presented by Anderson *et al.* (1973) and published parameters for similar materials from Nixon (1991).

TABLE 2: Material Properties Used in the Thermal Models

Material	Moisture Content (%)	Dry Density (t/m^3)	Specific Gravity, Gs (t/m^3)	Void ratio, e	Porosity, n (%)	Initial Degree of Saturation (%)[1]	Initial Volumetric Water Content[1]	Initial Thermal Conductivity [1] (W/m °C)		Volumetric Heat Capacity [1] (MJ/m^3 °C)	
								Frozen	Thawed	Frozen	Thawed
Rockfill saturated	15.7	2.15	3.2	0.49	32.8	100	0.328	2.6	1.8	2.2	2.9
Rockfill unsaturated	1.0	2.15	3.2	0.49	32.8	6.6	0.02	0.75	0.75	1.0	1.0
Filter	5.0	1.9	2.89	0.52	34.3	27.7	0.095	2.0	1.4	1.6	1.8
Till	16.6	1.87	2.71	0.45	31.0	100	0.31	2.4	1.8	2.0	2.6
Fractured bedrock	0.5	2.71	3.0	-	-	100	0.05	2.7	2.7	2.7	2.7
Bedrock	0.5	2.71	3.0	-	-	100	0.005	2.9	2.9	2.5	2.5
Tailings	39.1	1310	3	1.29[2]	56.3	100	0.51	2.9	1.9	2.1	3.0

[1] Variation in the degree of saturation and volumetric water contents at different time steps are obtained from the Seepage component of the model. The thermal conductivity and volumetric heat capacity are then adjusted by the TEMP/W solver.

[2] The tailings are expected to consolidate with time and reach an average void ratio of 1 or less. Sizing of the impoundment was made considering progressive tailings consolidation and allowance was made for ice entrapment.

Sensitivity of Tailings Thermal Properties

As described in Section 2, the thermal conductivity of the tailings may vary in the field associated with changes in the tailings density and water content associated with tailings segregation and consolidation. Sensitivity analyses were performed to assess the impact of these parameters in the tailings freezing process. For saturated samples, higher thermal conductivity values will occur at dense states and low volumetric water content values. High thermal conductivity values increase the rate at which heat can move and be extracted from the tailings.

The sensitivity analyses were carried out using a 1D model composed of 38 m of tailings underlain by 24 m of bedrock, and run for a period of 18 years, which comprises 8 years of deposition followed by 10 years after mine closure. The tailings deposition temperature was assumed as 10^{o}C, and the calculated ground surface temperature function described in Section 4.3 was used as the upper boundary condition for the models and the temperature of foundation at 24 m depth was set constant at 2.3^{o}C as indicated by on site thermistors. The sequence of tailings elevation modeled during deposition followed the Tailings Deposition Plan described in Section 4.4.

Initially, the sensitivity analyses compared the model results obtained using the laboratory measured tailings thermal conductivity values (Table 1), to the results from the adjusted tailings thermal conductivity values presented in Table 2. Figure 1 shows the depth of the freezing front computed for both set of thermal conductivity values 10 years after mine closure.

The depth of the freezing front 10 years after the mine closure that was computed using the laboratory measured tailings thermal conductivity is about 1.4 m deeper than the position of the freezing front computed using the adjusted lower thermal properties. The tailings specimen tested in the laboratory was denser than expected to occur in field and therefore, the measured thermal conductivity values should be considered as the upper bound of the tailings thermal conductivity range when the tailings consolidate to the maximum density.

The sensitivity analyses also compared the tailings temperature profiles computed for tailings with increasing volumetric water contents. Changes in the tailings volumetric water content may occur associated with ice entrapment (increasing the overall water content), or variation in tailings density related to tailings consolidation, or deformation under self weight or in response to the placement of a rock cover (leading to lower volumetric water contents).

The water content will affect the length of time the temperature remains at the freezing point (zero curtain effect). This length of time is directly related to the latent heat that is released so, the higher the water content, the more latent heat and the longer it takes to be removed. Figure 2 shows the computed temperature profiles at the end of deposition and 10 years after closure for tailings with volumetric water content of 42.0 %, 51 % (design value) and 61.0% (or 24.9 %, 39.1 % and 52.1 % by mass), all cases using the adjusted tailings thermal properties presented in Table 2.

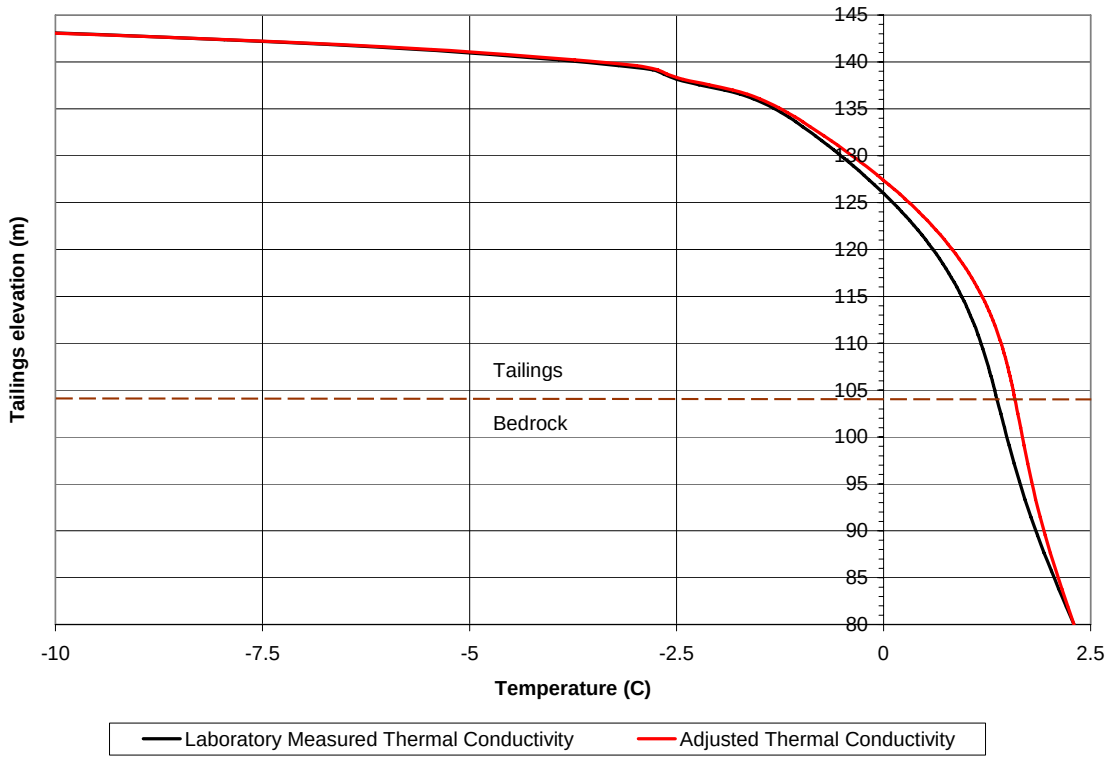

Figure 1 – Computed Depth of Freezing Front 10 Years after Operations Using the Tailings Thermal Conductivity Measured in the Laboratory and the Adjusted Values

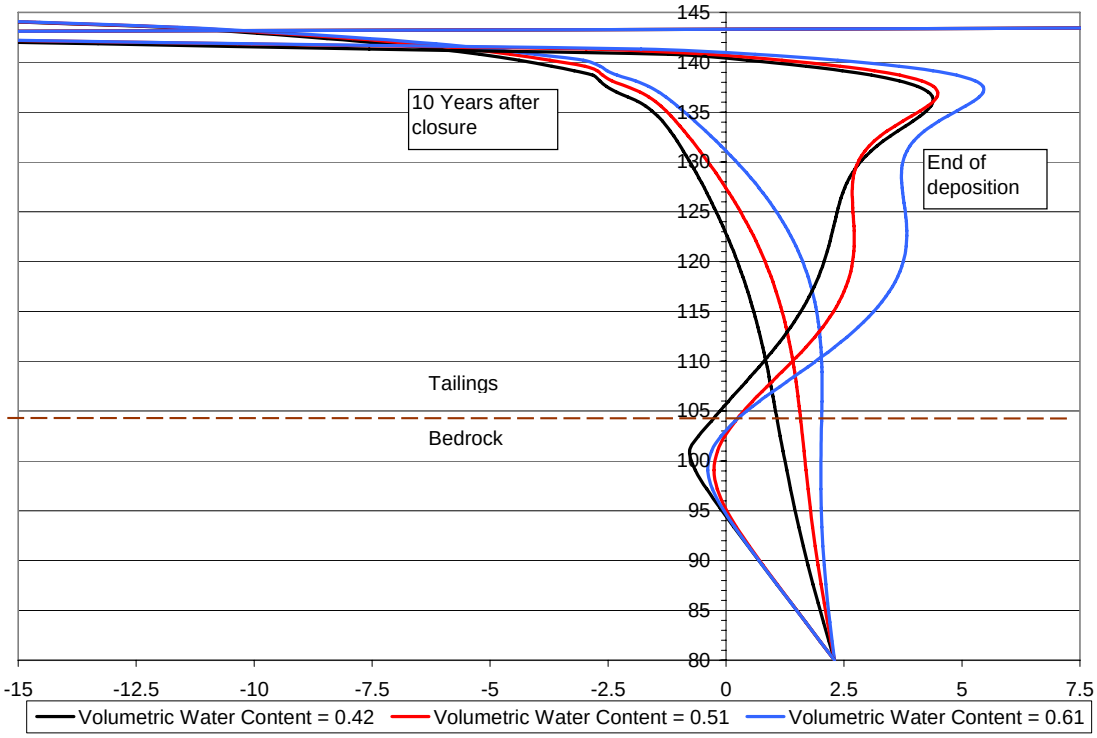

Figure 2 – Temperature Profile of Tailings Ten Years after Closure with Varying Volumetric Water Content

From Figure 2, it becomes evident that the water in the tailings will play an important role in the freezing process. The difference in depth of the freezing front 10 years after closure computed for the two extreme values of volumetric water contents (0.42 and 0.61) is about 8.5 m. The lower volumetric water content bound was taken from the Proctor test carried out during the thermal conductivity measurements, and would then be associated with highly consolidated tailings. On the other hand, the upper bound could represent zones with ice trapped during deposition that could eventually thaw as the heat exchange between old and fresh tailings proceeds during the deposition phase.

As described in Section 2, it is likely that segregation during deposition causes tailings adjacent to the spigot and dike to be denser and present lower water contents than tailings material remote from the spigot and dike. From Figures 1 and 2, it is expected that this portion of denser tailings will freeze faster than tailings located in the central area of the TSF.

4.2.2 Hydraulic Properties

Table 3 presents the hydraulic conductivity values used in the seepage component of the coupled analysis.

TABLE 3: Hydraulic Conductivity Values Used in the Models

Material	Hydraulic Conductivity Range Observed (m/s)	Modeled Hydraulic Conductivity Value (m/s)	Source
Rockfill/Filter	n/a	$1x10^{-2}$	Experience with similar materials
Native Till Layer and Till Backfill	$3x10^{-4}$ - $1x10^{-7}$	$1x10^{-6}$	Falling head tests from Dec 2002 geotechnical testing.
Fractured bedrock (upper 20 m of bedrock)	$1x10^{-4}$ and $3x10^{-9}$	$5x10^{-6}$	Previous 2002 and 2003 geotechnical field investigations
Grouted Bedrock	n/a	$1x10^{-7}$	Previous 2002 and 2003 geotechnical field investigations
Bedrock	$1x10^{-8}$	$2x10^{-7}$	BH 03GT-GI-6 packer tests BH 03GT-GI-3 packer tests Previous 2002 and 2003 geotechnical field investigations
Portage Fault	$1x10^{-5}$	$1x10^{-5}$ to 70 m depth and $5x10^{-6}$ below	Golder (2007a)
Tailings	$3x10^{-5}$ and $7.6x10^{-9}$	$5x10^{-7}$	Previous 2002 and 2003 geotechnical field investigations
Coletanche Liner	$< 10^{-11}$ m/s	Impermeable	Design specification.

4.3 Estimation of Ground Surface Temperature

4.3.1 Climate Data Review

New climate data have not been available since the work done early in 2007. Climate data was obtained from a weather station at the mine site for the period between September 1997 and December 2005. Daily climate data were available from September 1997 to September 2003, and mean monthly data were available for the period between September 2003 and December 2005. To assure higher precision in the calculated surface temperature function, only daily data have been used for this study, and these are presented in Figures 3 and 4.

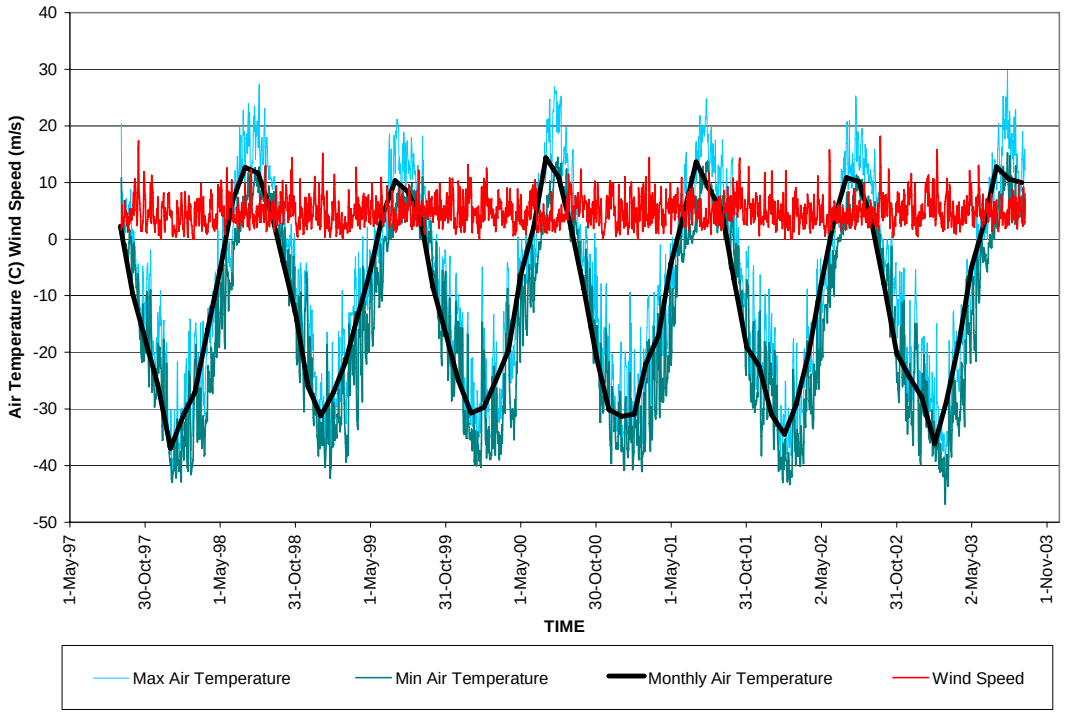

Figure 3 – Air Temperature and Wind Speed Data

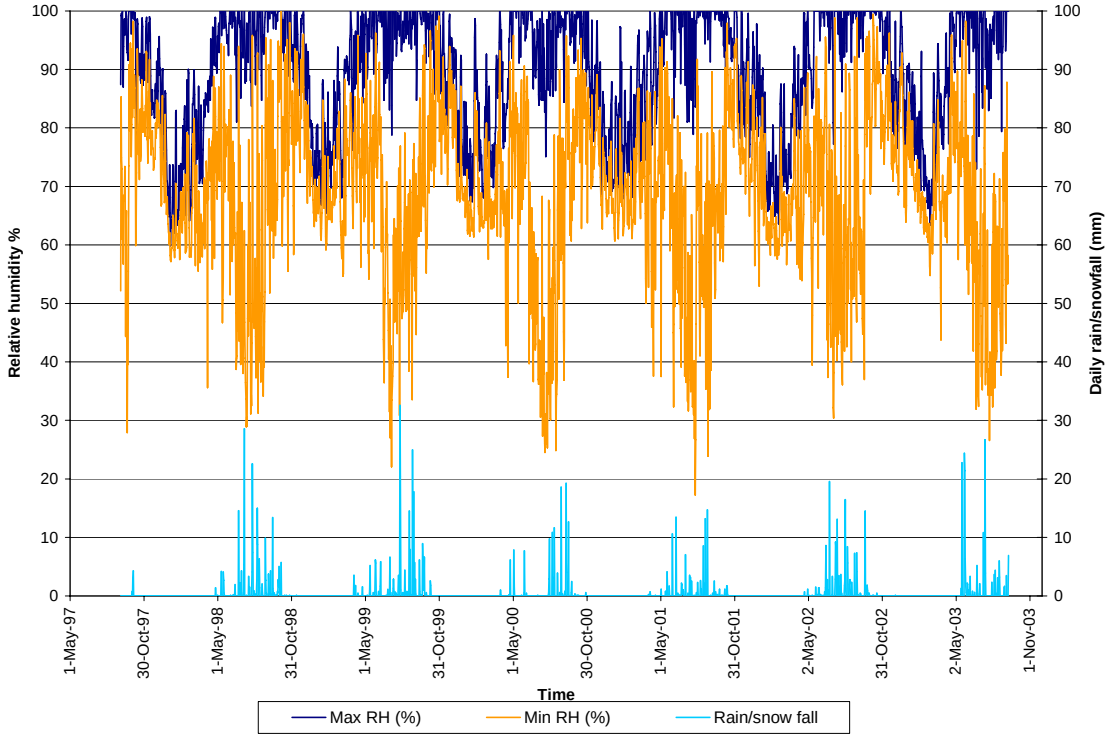

Figure 4 – Total Precipitation and Relative Humidity

4.3.2 Ground Temperature Estimation

The climate information was used to perform numerical model analyses with TEMP/W, which uses a rigorous approach to calculation of ground temperature. The model covered a period of 6 years between September 1997 and September 2003.

The calculated ground surface temperature was averaged to general monthly values as shown on Figure 5. In addition, the six-year period data was averaged by month to generate a general annual ground surface temperature function as shown on Figure 6. Figure 6 also shows the mean air temperature from the daily data between 1997 and 2003, the mean air temperature incorporating the monthly data available between 2003 and 2005, and the reported mean soil temperatures in 2005 at about 0.3 m depth.

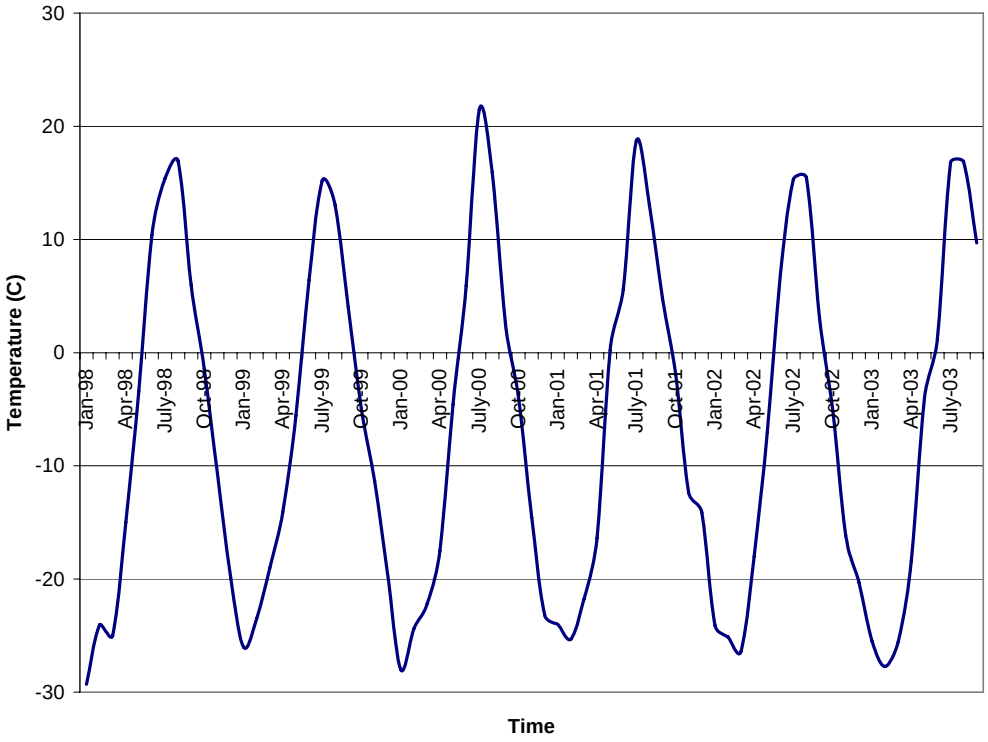

Figure 5 – Calculated Ground Surface Temperature

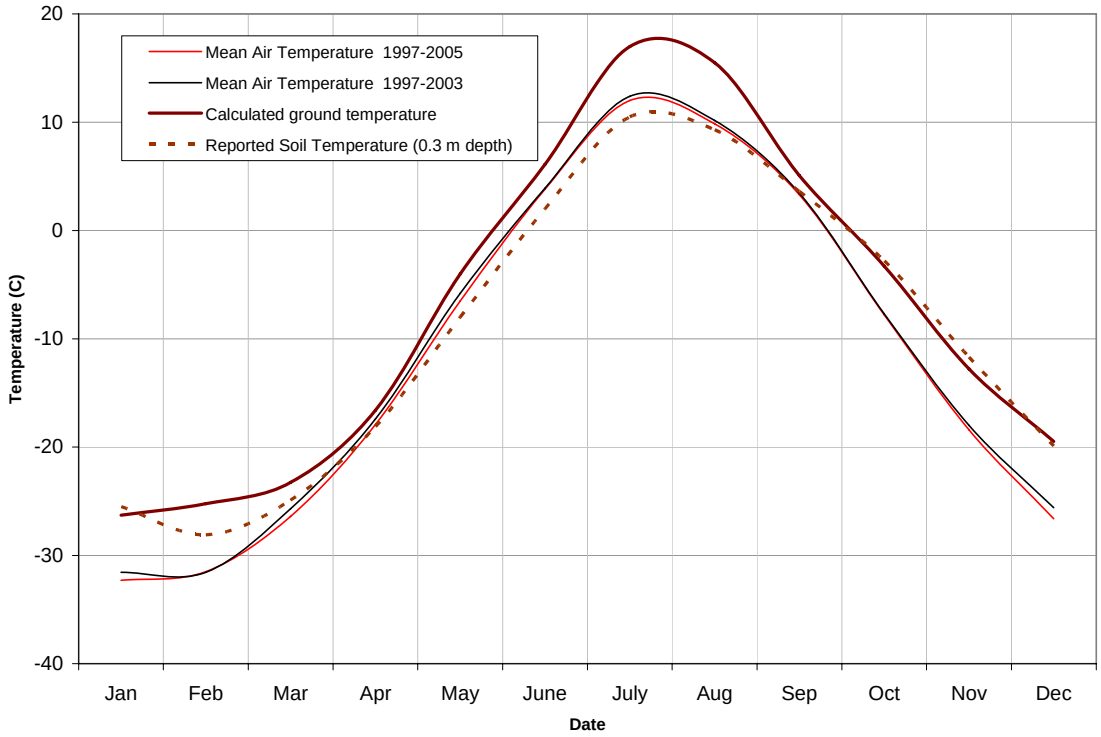

Figure 6 – General Ground Surface Temperature Function

The generated ground temperature curve agrees well with the reported soil temperatures in the winter period, but shows warmer temperatures during the summer period. It must be noted that the sensor that measured the soil temperature was reported to be at about 0.3 m depth, and so temperatures should in fact be cooler than surface in summer times.

4.3.3 Validation of the Ground Surface Temperature Function

The general ground surface temperature function was validated through a 1-D model consisting of 4 m of till overburden underlain by 40 m of bedrock, and covering a period of 1.5 years. The computed temperature profiles were compared to measured profiles obtained from the thermistor 03GT-TD-1, which was drilled to a depth of 44 m and is located away from the influence of the lake in the proposed north abutment of the Central Dike.

The temperature profile measured on April 17, 2005 was taken as the starting reference temperature profile, and the model ran until July 17, 2006. Figure 7 shows the measured and computed temperature profiles within the modeled period.

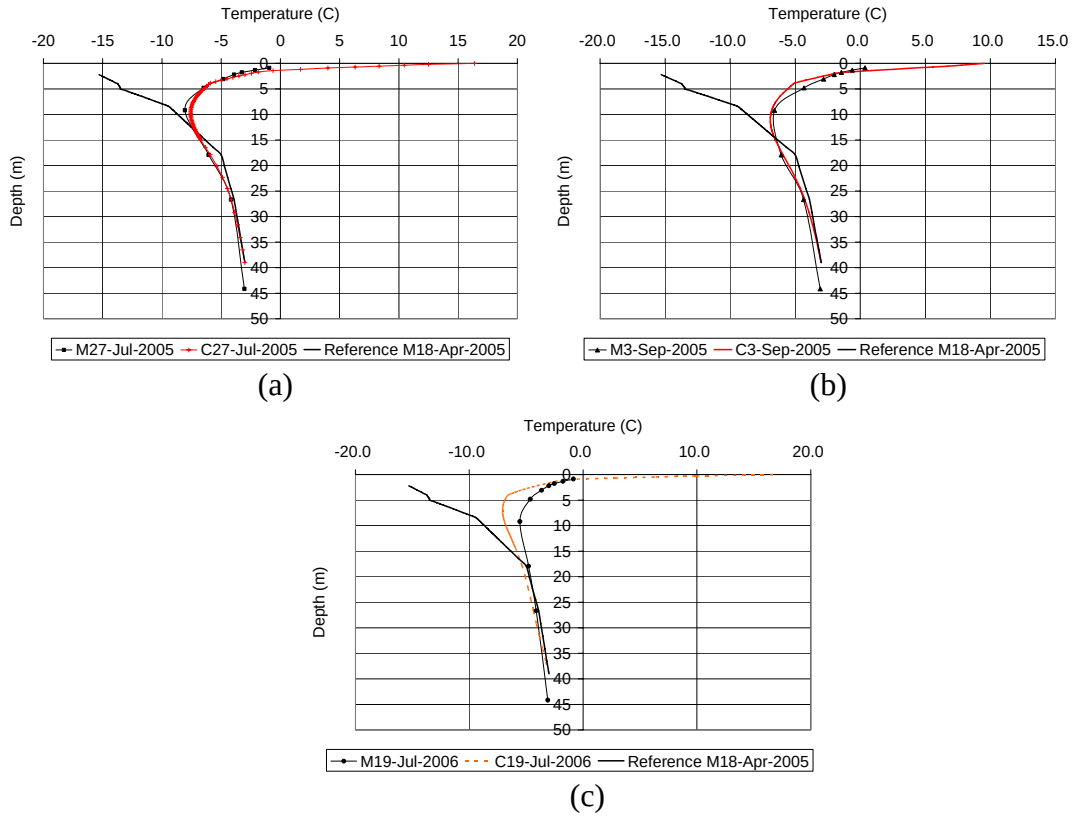

Figure 7 – Comparison between measured (M) and computed (C) temperature profiles at different times (Reference borehole 03GT-TD-1).

The computed temperature profiles using the general ground surface temperature function agreed well with the 2005 measured profile and a broader variation was observed for the July 2006 profiles. However, a perfect match of computed and measured profiles with time is not possible to obtain because of deviations related to year-to-year climate specifics.

The ground surface temperature function that was generated for this study was intended to represent the average ground surface temperature and, combined with the estimated thermal properties of the foundation materials, resulted in temperature profiles that are compatible with field measurements. Therefore, the ground temperature function generated for this modeling exercise is considered to be appropriate.

4.4 Tailings Deposition Sequence

The modeled sequence of tailings deposition was based on the proposed tailings deposition plan for the southern basin, with tailings rising from elevation 104 m to 143.5 m over a period of six years. A summary of the tailings deposition plan as designed for a reference spigot (Spigot 5) is presented in Table 4.

TABLE 4: Tailings Deposition Sequence at Spigot 5 (Extracted from the Tailings Deposition Plan)

Start Date	End Date	Days (Accum.)	Tailings Surface Elevation (m)	Pond Elev. (m)
1-Feb-09	2-Mar-09	31	108.0	107.7
6-Nov-09	24-Dec-09	328	117.7	116.5
23-Jun-10	21-Jul-10	536	122.7	121.3
26-Aug-10	3-Oct-10	611	124.3	122.7
3-Nov-10	15-Dec-10	684	125.8	124.1
19-Jun-11	21-Jul-11	901	129.5	127.6
18-Aug-11	3-Oct-11	976	130.8	128.7
5-Nov-11	19-Dec-11	1,053	132.0	129.8
31-May-12	3-Jul-12	1,250	134.4	132.0
3-Aug-12	11-Sep-12	1,319	135.3	132.7
3-Nov-12	18-Dec-12	1,417	136.5	133.8
23-Jun-13	3-Aug-13	1,646	138.5	135.7
15-Sep-13	29-Oct-13	1,733	139.3	136.3
16-Dec-13	2-Feb-14	1,828	140.3	137.5
4-Aug-14	28-Sep-14	2,066	142.3	138.9
6-Feb-15	14-Mar-15	2,234	143.5	140.1

The rate of tailings rise is a function of the spatial distribution of the spigots, the rate of tailings production, size of deposition areas and local topography. For a specific portion of the tailings area, tailings elevation will rise mostly during the time deposition is made from spigots located in or near this area, and should be less affected by deposition from spigots located far away.

In terms of the dynamics of heat exchange during deposition, newly deposited warm tailings will continuously heat previous lifts of tailings. When deposition is moved to another sector, the heat source ceases and the tailings start to cool in response to exposure to the on-average cooler air temperature. It may also happen that an inactive sector will receive tailings from nearby active sectors, and the tailings will also contribute heat to previously deposited tailings.

To assess the impact of this dynamic process in the evolution of tailings temperatures three scenarios were modeled:

1. Tailings increase elevation only during the sector's active discharge period and are exposed to air temperature during the entire sector's inactive time,

2. Tailings increase elevation during the active period of the nearest spigot plus 25 % of the inactive period, representing migration of tailings from an active sector. As a result, the air-exposure period is reduced to 75% of the sector's inactive time, and,

3. Tailings increase elevation during the sector's active period, and extend for 50 % of the inactive time, representing greater tailings migration from adjacent active sectors. Tailings exposure time to air temperature is then reduced to 50% of the sector's inactive time.

The main impact of modeling the migration of warm tailings into an inactive sector is that the length of time in which tailings are directly exposed to the air temperature between two subsequent periods of deposition is shorter. In addition, with migration of tailings from active to inactive sectors, the thickness of fresh deposited tailings in a sector will increase. The shorter the period the tailings are exposed to the cooler air temperature, the shallower will be the frozen portion before another lift of warm tailings is deposited, and the overall tailings temperature will tend to be warmer at the end of operations.

4.5 Models Configuration

4.5.1 Tailings Model

As described above, the tailings temperature profile at the end of deposition will be a result of the combination of cyclic warming and cooling periods. For modeling purposes, warming periods are related to direct deposition of tailings into an active sector plus migration of warmer tailings from active to nearby inactive sectors. The models assume that cooling occurs during the inactive periods of a sector and when migration of fresh tailings from active sectors is limited. Figure 8 shows the warming and cooling cycles modeled for the three scenarios described above.

Each stage of tailings elevation is modeled for one warming and one cooling cycle before the tailings elevation is increased for the next stage. In total, each scenario modeled is composed of 15 stages of increasing tailings elevation, and 31 warming and cooling cycles. Figure 9 shows a scheme of the modeling sequence from Stage 1 to Stage 3 for Scenario 2, showing thermal and hydraulic boundary conditions and how the warming and cooling cycles were applied. The modeling sequence continued to Stage 15, until the tailings reach its final modeled elevation as showed in Figure 10.

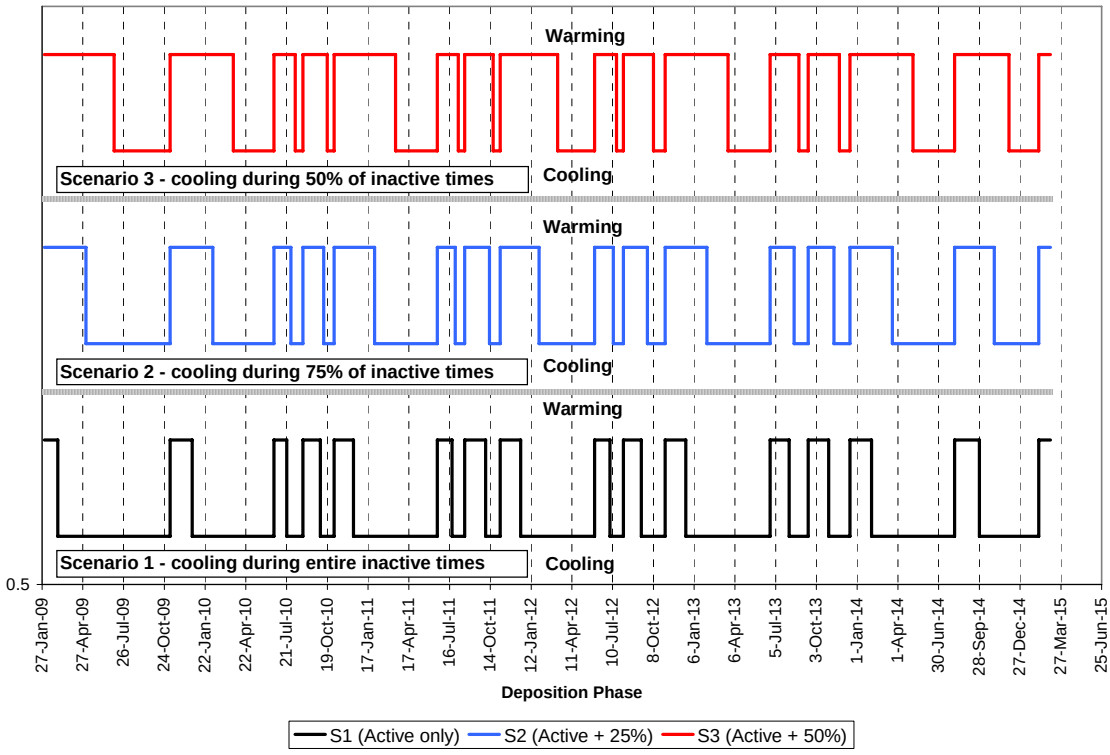

Figure 8 – Warming and Cooling Cycles during Deposition for the three Scenarios Considered.

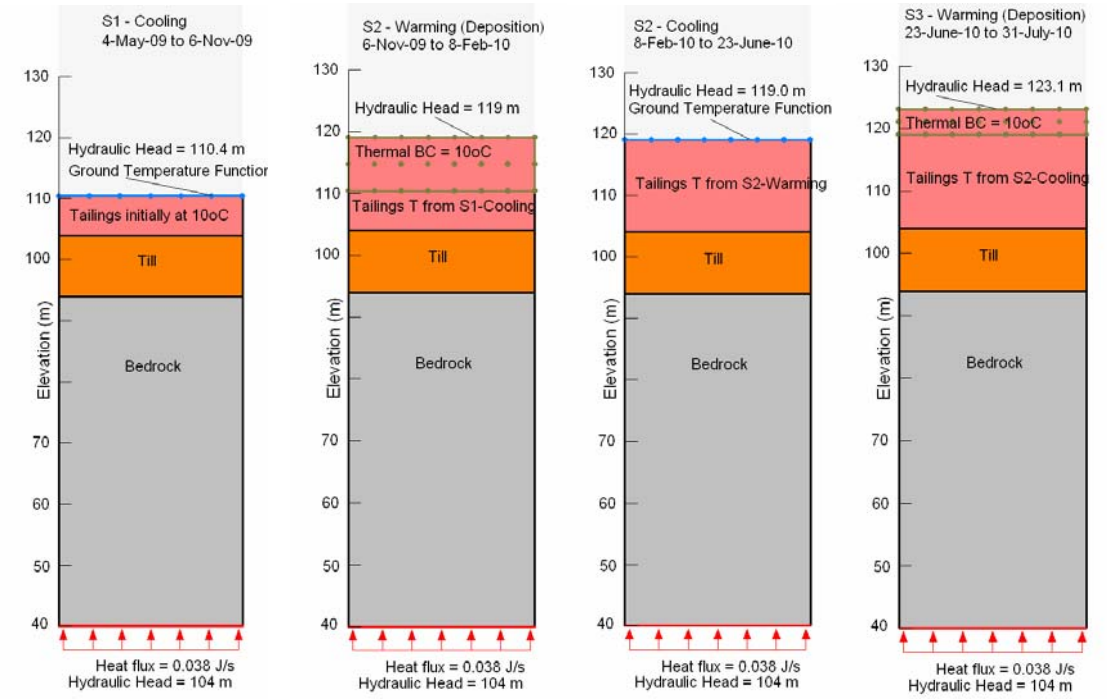

Figure 9 – Example of Tailings Modeling Sequencing and Boundary Conditions. Models Continued to Stage 15.

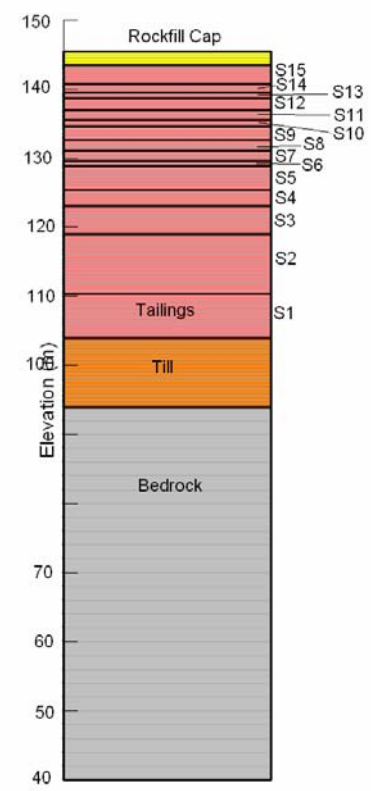

Figure 10 – 1-D Tailings Model Sequencing with Tailings Elevation Increasing in 15 Stages.

As shown in Figures 9 and 10, the models had a 1-D configuration and were composed of 15 stages, with the final temperature profile and flow velocities computed for each stage being applied as the initial temperature profile for the subsequent stage. The initial foundation temperatures prior to tailings deposition was estimated through a simplified model, which indicated that one year after the lake drawdown, the frozen layer would develop to a depth of 3.0 m. The initial temperature of the bedrock at 60 m depth was assumed to be 3.0 ^{o}C, based on site thermistors.

The sequential models followed the tailings deposition sequence presented in Table 4, with adjusted warming and cooling stages in accordance to the different scenarios modeled as shown in Figure 8. During cooling cycles, the ground surface temperature function described in Section 3.3 was applied to the upper boundary condition of the models, while during warming cycles the upper boundary condition was defined as the average tailings deposition temperature. Sensitivity analyses considered the average tailings deposition temperature as 5 ^{o}C, 10 ^{o}C, 15 ^{o}C and 20^{o}C.

A geothermal flux of 0.038 J/s (0.013 ^{o}C/m), calculated from on site thermistors, was used as the lower boundary condition of the models.

As for the seepage component of the analyses, the water table was assumed to be initially at the base of the tailings, and the hydraulic gradient increased as the tailings elevation increased. The upper boundary condition for the different stages was defined as a constant head equal to the tailings elevation at each stage. A constant head of 104 m was assigned as the lower boundary condition to all models

4.5.2 Tailings Storage Facility Model

The Tailings Storage Facility was modeled using a coupled seepage/thermal 2-D model that incorporated the tailings area, Central Dike, Portage Pit and the lake. The model was subdivided into two phases: Phase 1 modeled the flooding of the Portage Pit with the lake level rising to the final elevation of 134.1 m during a period of 4 years and, Phase 2 modeled the TSF in the long term up to 100 years after closure. The model initial conditions derived from simplified separate models as follows:

Initial water table position: A separate seepage analysis was performed to compute the position of the water table at the end of deposition. The model considered the water table at elevation of 146 m on the surface of tailings, and a review by pressures boundary was applied to the wall of the Portage Pit.

Foundation and Dike initial temperatures: The initial temperature of the foundation beneath the Dike after the lake drawdown was estimated through a separate simplified thermal model. This used the ground surface temperature function as the upper boundary condition and the measured deep foundation temperature as the lower boundary condition. The model covered a period of eight years to represent freezing of the foundation during operations. The temperature of the foundation beneath the tailings was taken from the 1-D tailings deposition model.

The several boundaries conditions applied to the coupled models derived from both field instrumentation data and the tailings 1-D models, and are presented in Table 5.

TABLE 5: Boundary Conditions Used in the Coupled Analysis

Model location	Stage 1 – Flooding of Portage Pit (year 0 – 4)		Stage 2 – Long Term (years 4 to 100)	
	Thermal	**Hydraulic**	**Thermal**	**Hydraulic**
Surface of rock cover over tailings	GTF*	Constant head: 146 m	GTF + 6.4^{o}C in 100 years	No BC
Dike above El. 134.1 m	GTF	No BC	GTF + 6.4^{o}C in 100 years	No BC
Dike below El 134.1 m and downstream portions	2 ^{o}C – below El. 80 m 4 ^{o}C – El. 80 to 134.1 m.	Head vs. Time function: El. 75 m to 134.1 m over 4 years	2oC – below El. 80 m 4oC – El. 80 to 134.1 m	Constant head: 134.1 m
Liner	-	Impermeable	-	Impermeable
Bottom of the model	Heat Flux: 0.038 J/s	No Flux	Heat flux: 0.038 J/s	No Flux

* *GTF = Ground Temperature Function*

Considerations to the Portage Fault

The Second Portage Fault is inferred to run beneath the North Arm of Second Portage Lake where the Tailings Storage Facility and Central Dike are located. Based on field investigations, the fault and associated fractured rock zone of higher permeability are typically 5 m wide and have a hydraulic conductivity of $1x10^{-5}$ m/s (Golder 2007a).

The fault alignment is near parallel to the representative cross section used to model the TSF, so the fault could not be directly included in a 2-D model together with areas located beyond the fault's limits. To assess the impact of the fault on the seepage rates that occur during and after operations, a cross section that exactly matches the fault orientation was modeled.

In this scenario, the hydraulic conductivity of the foundation down to about 70 m in depth was assumed to be the same as the fault (*i.e.*, $1x10^{-5}$ m/s). The hydraulic conductivity of the fault zone is likely to reduce in depth associated with higher pressures so the hydraulic conductivity of this deeper portion was assumed to be similar to the fractured bedrock (*i.e.*, $5x10^{-6}$ m/s).

The total flow through the fault zone is then calculated by multiplying the computed flux rates by the average fault width of 5 m. The total flow rate for the entire facility is calculated combining the flow rates obtained for the fault and intact materials.

5.0 CONTAMINANT TRANSPORT MODEL

In addition to the coupled temperature/seepage models, a separate model was prepared to evaluate the process of transport of contaminants from the tailings area toward the Portage Pit. Preliminary water quality tests indicated that the main contaminants of concern will be arsenic, copper, lead, zinc, nickel and total cyanide. (Golder 2007c).

The model was developed using the 2-D code CTRAN by Geoslope Inc, which models both the movement of the contaminant with the flowing water and the apparent mixing and spreading of the contaminant within the flow system. The contaminant model is semi-coupled with the 2D seepage/temperature models described above, and therefore uses the same geometry.

As will be discussed in the next section, the coupled seepage/temperature models indicated that the upper foundation of the tailings will be frozen during operations and shortly after the mine closure, but will then thaw upon continuing heat exchange with warmer tailings and foundation located above and beneath the frozen portion. The contaminant model uses the flow velocities computed from the 2D seepage/temperature models to perform the advection/dispersion contaminant analysis, and assumed that contaminants would not be transported during operations due to water flow restrictions associated with the frozen foundation. The model assessed the evolution of the contaminant plume after closure, when the foundation was predicted to thaw.

A sensitivity analysis was done to evaluate what the transport of contaminant would be if the foundation remains thawed during operations, resulting in transport of contaminants occurring together with the tailings deposition. For this analysis, the flow velocities during operations were computed through a separate 2D seepage analysis considering that the water table in the tailings rises from 104 m to 146 m over a period of 8 years. The flow velocities after closure were computed considering the rise of the Portage Pit Lake and decreasing water table in the tailings associated with the tailings drain down process.

As the identified target contaminants present different concentrations, their concentrations were normalized so that a single analysis could be used to produce a general picture of the contaminant transport process. Therefore, it was defined that the tailings would present a unit mass contaminant concentration of 1 kg/m^3 (1 mg/l).

The effective diffusion coefficient of the foundation was assumed as $1x10^{-10}$ m^2/s, which is one order of magnitude lower than the reported diffusion coefficient of most contaminants in water bodies, but consistent with diffusion in groundwater (Fetter C. 2001). The longitudinal and transversal dispersivity through the foundation was defined as 10 m and 1 m, respectively. The contaminants were assumed not to be attenuated by the foundation and therefore no contaminant decay was applied.

6.0 MODEL RESULTS

6.1 Tailings Model

6.1.1 End of Deposition Temperatures for Different Scenarios

As discussed above, the evolution of tailings temperature during deposition will depend upon several factors such as: deposition temperature, deposition sequencing, duration of active and inactive periods and potential migration and spreading of tailings during deposition. Figures 11 to 13 show the computed temperature profiles of tailings at the end of deposition for the three different scenarios modeled and for different average tailings deposition temperatures. In addition, the tailings temperature profile used in the 2D TSF model is also shown in each figure.

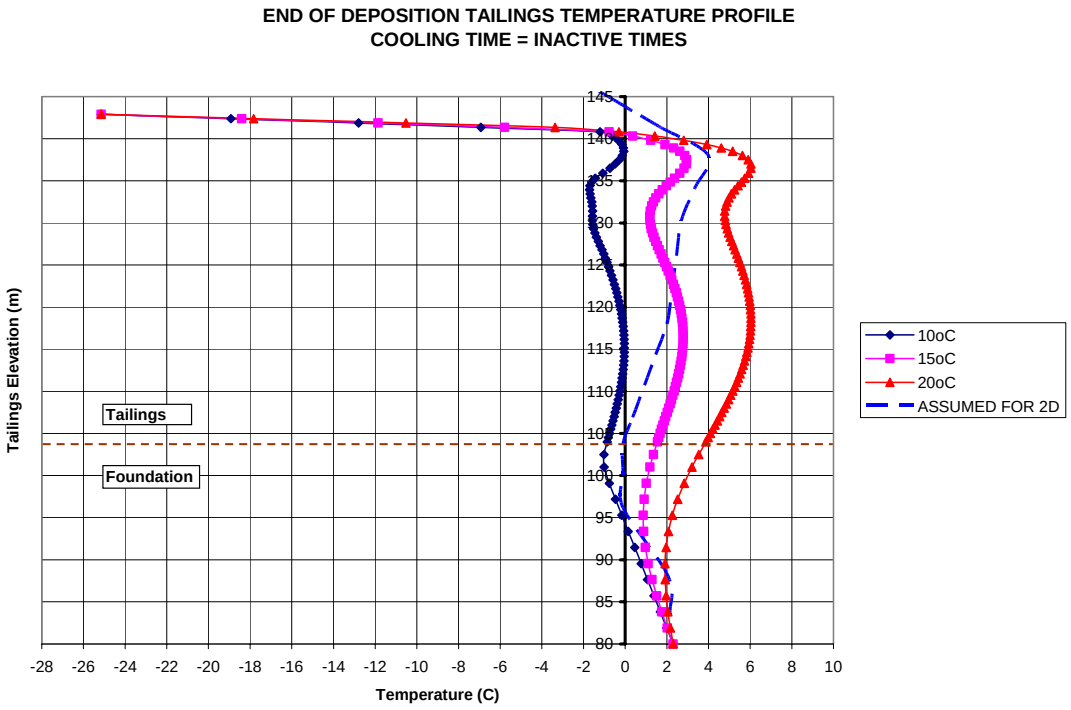

Figure 11 – Computed Tailings Temperature at the end of Deposition for Scenario 1 (Cooling Times Equal Inactive Times) with Different Tailings Deposition Temperatures

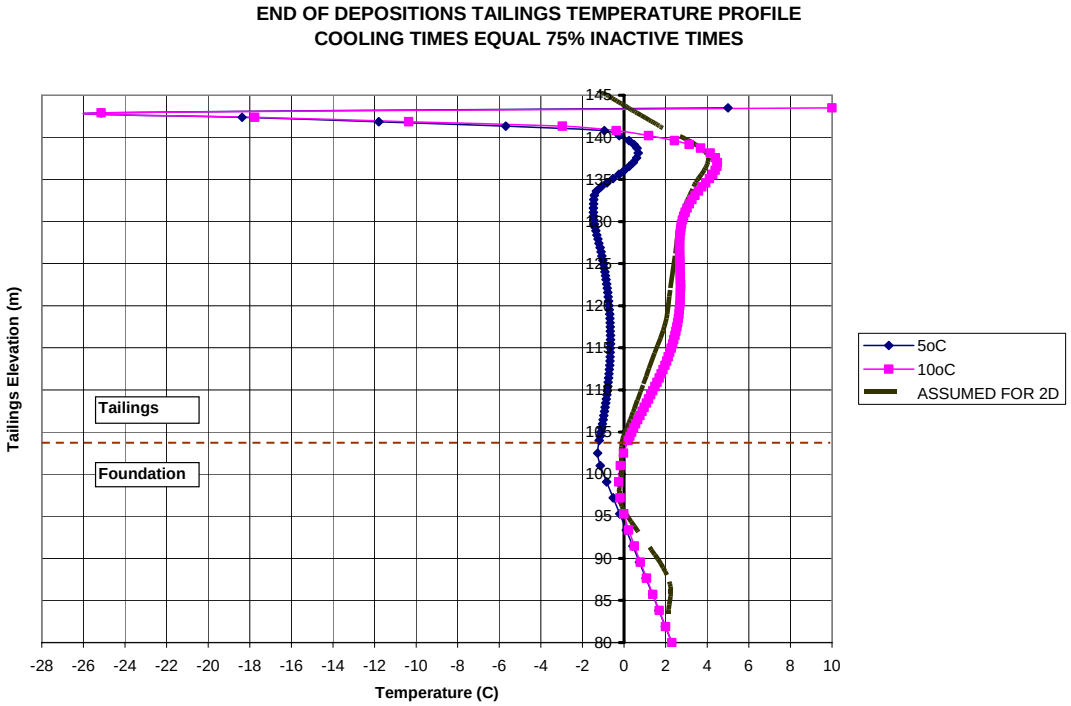

Figure 12 – Computed Tailings Temperature at the end of Deposition for Scenario 2 (Cooling Times Equal 75% Inactive Times) with Different Tailings Deposition Temperatures.

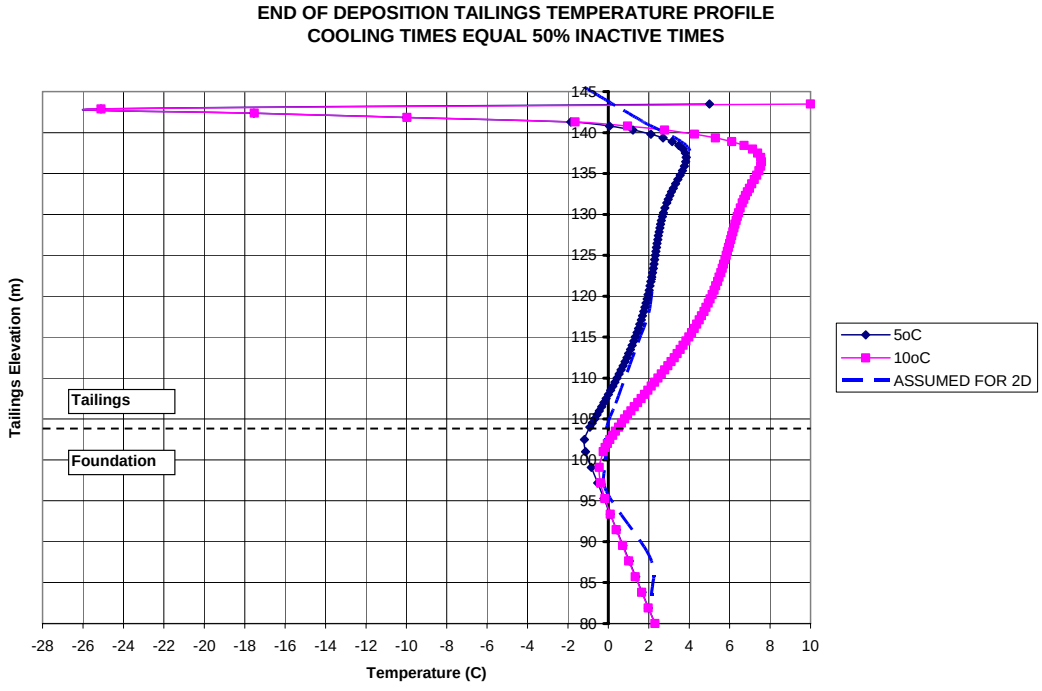

Figure 13 – Computed Tailings Temperature at the end of Deposition for Scenario 3 (Cooling Times Equal 50% Inactive Times) with different Tailings Deposition Temperatures.

As shown in the figures, the models indicated that the final tailings temperature profile will be warmer for higher deposition temperatures and shorter cooling periods. The temperature profile at the end of deposition computed for Scenario 2 (cooling period equals 75% of inactive times) and at tailings deposition temperature of 10^{o}C was used in the 2-D long term Tailings Storage Facility model.

The chosen temperature profile is similar to the temperature profile computed for Scenario 1 (cooling period equals inactive times) for average tailings deposition temperature of 15^{o}C, and matches Scenario 3 (cooling period equals 50% inactive times) for tailings deposition temperature of 5^{o}C.

The chosen final tailings temperature profiles can be considered conservative because the loss of heat from the tailings during deposition is not directly incorporated in the models. As described before, the tailings temperature was set to be constant during deposition periods. In reality, heat exchange between fresh deposited tailings and the air temperature occurs during all times, and the tailings actual temperature will in fact vary during deposition depending on daily air temperature as well as heat dissipation as the tailings flow away from the spigots.

From Figures 11 and 12, it can be seem that, if the average tailings temperature during deposition becomes less than 10^{o}C (associated with steady heat loss processes), the models indicated that the entire tailings body would be nearly frozen by the end of deposition for scenarios 1 (cooling times equal inactive times) and 2 (cooling times equal 75% inactive times), which would imply essentially no water flux or contaminant transport from the tailings area.

6.1.2 Evolution of Temperatures During Deposition

Figure 14 shows the evolution of temperature in the tailings column at different times during deposition for the selected scenario 2, with tailings deposition temperatures of 10^{o}C. Figure 15 shows the evolution of tailings temperature with time at different elevations in the tailings.

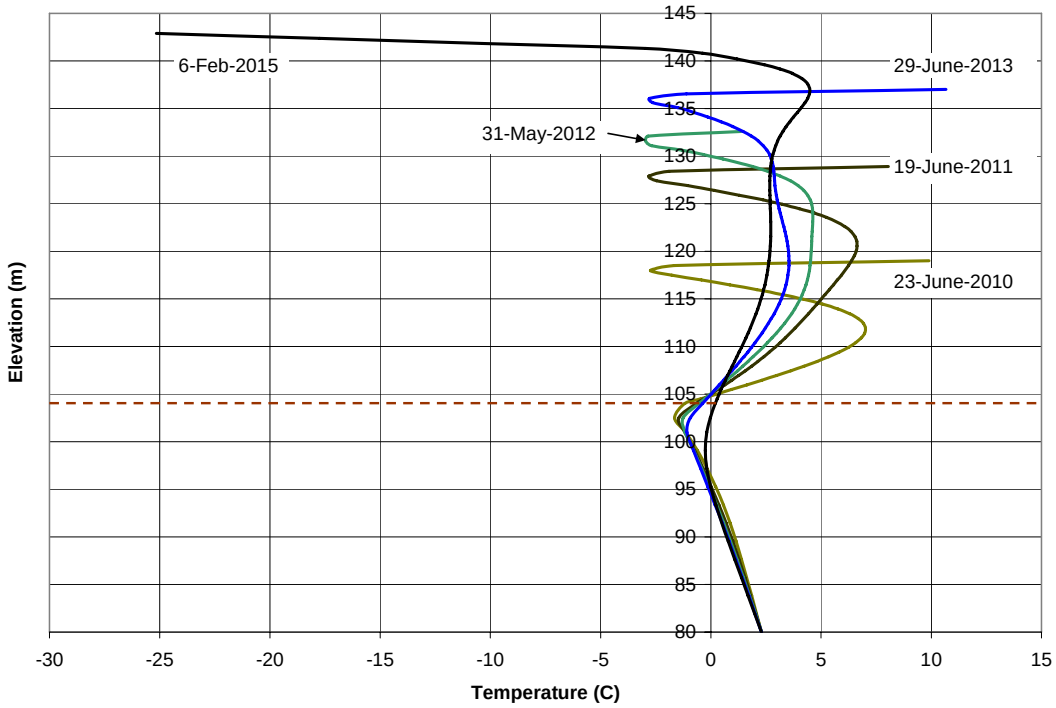

Figure 14 – Computed Temperature Profiles of Tailings at Increasing Elevations at Different Times during the Deposition Phase.

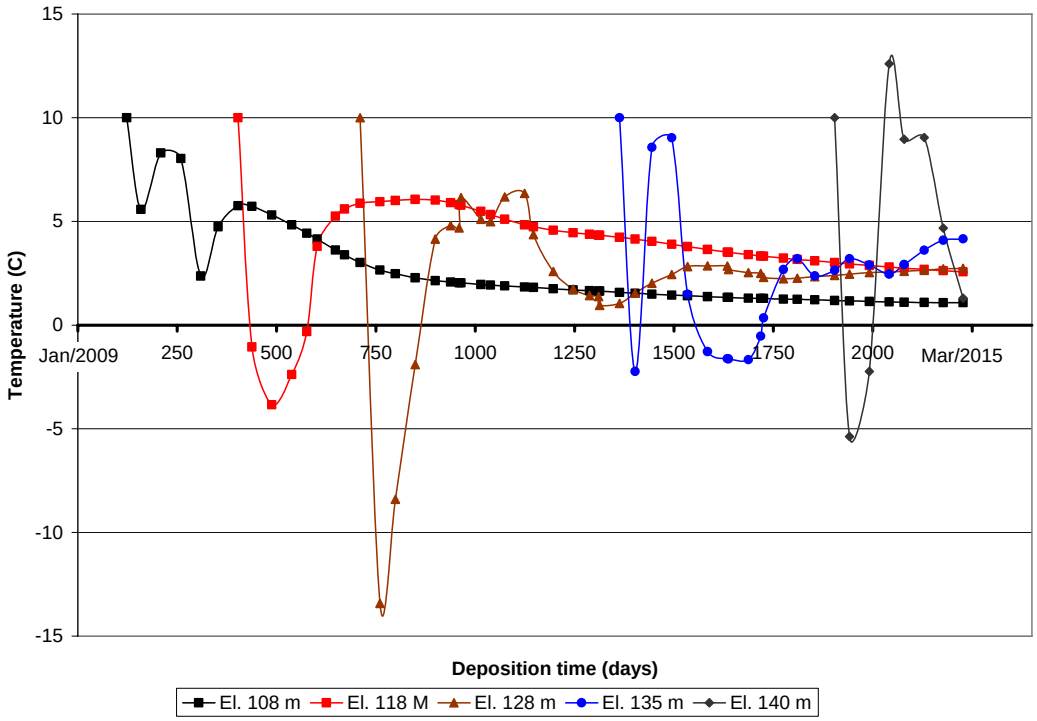

Figure 15 – Evolution of Tailings Temperature with time at Different Elevations of the Tailings Column.

Figures 14 and 15 show that the temperatures within the tailings body during deposition are constantly changing in response to warming and cooling cycles associated with active and inactive deposition times. The upper portion of tailings that freezes during cooling times, later becomes thawed upon deposition of a new lift of warm fresh tailings. As deposition continues, the tailings body becomes thicker, and the deeper portions of tailings are no longer significantly affected by warmer fresh tailings deposited on top. As a result, the overall tailings temperature is gradually reduced.

6.1.3 Influence of Water Flow

The influence of water flow on the tailings temperature profile is not expected to be large because of the low hydraulic conductivity of the tailings. In addition, the hydraulic conductivity of frozen tailings is even lower, causing the flow velocities to reduce markedly. Figure 16 and 17 show the temperature profiles computed for deposition scenario 2 at the end of deposition and 10 years after closure, and with and without consideration of water flow.

The models indicated that water flow carries heat within the tailings body causing the lower portion of the tailings and upper foundation to be about 0.3^{o}C warmer than when water flow is not considered. In spite of the apparent low variation, this difference in temperature associated with continuing water flow would cause the freezing front to be approximately 1.4 m shallower 10 years after closure. However, water flow will be greatly reduced in the long term due to freezing of tailings and reduction of hydraulic gradients upon flooding of the Portage Pit area. Therefore, the influence of water flow in the long term behavior of tailings is considered not to be important.

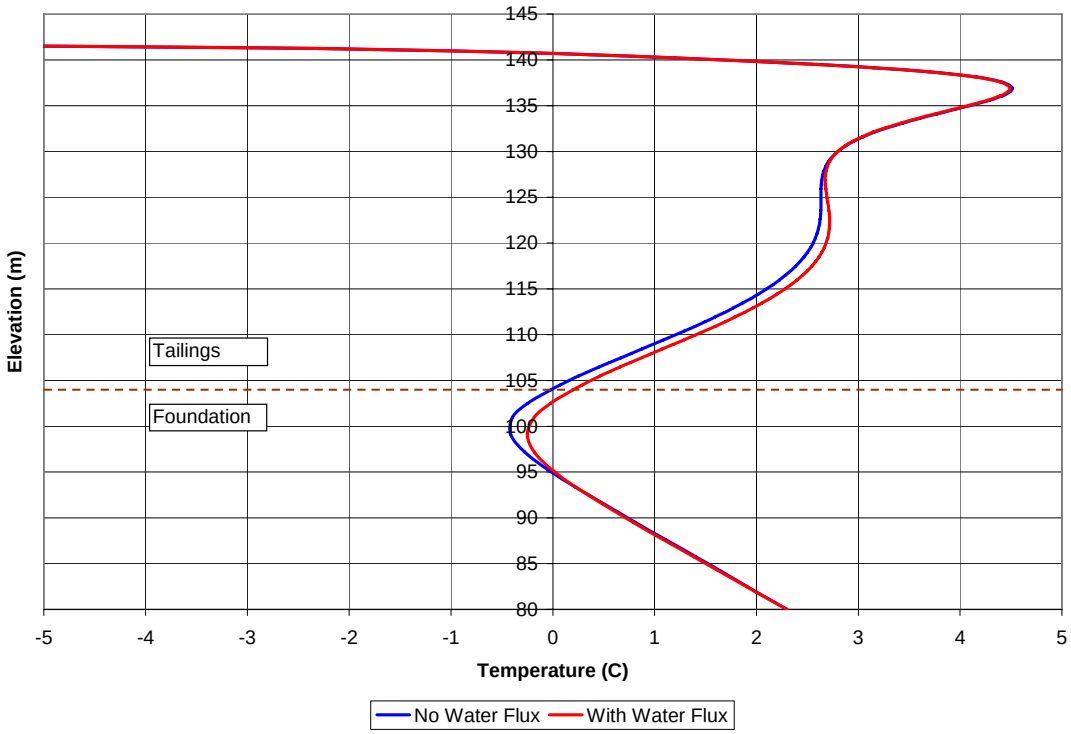

Figure 16 – Computed Tailings Temperature Profiles at the end of Deposition with and without Consideration to Water Flux.

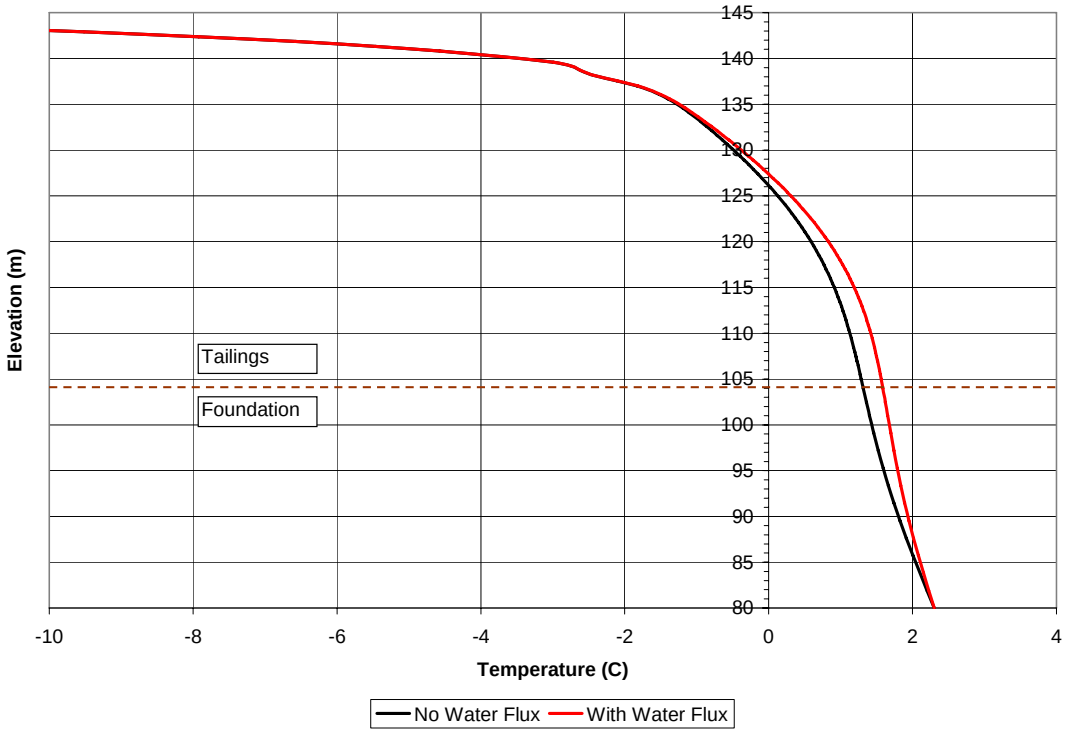

Figure 17 – Computed Tailings Temperature Profiles 10 years after Closure with and without Consideration to Water Flux.

6.2 Tailings Storage Facility Model

The evolution of temperatures and flow rates in the Tailings Storage Facility after the end of operations was evaluated considering a linear lake rise during a period of 4 years. In addition, long term analyses after completion of the Portage Pit flooding were developed for a period of 100 years.

6.2.1 Evolution of Temperatures

Figure 18 shows the computed temperature profiles in the tailings and foundation with time after closure. Figures 19 to 24 show the computed temperatures in the TSF area up to 100 years after the end of operations with ground temperature rising 6.4°C associated with global warming.

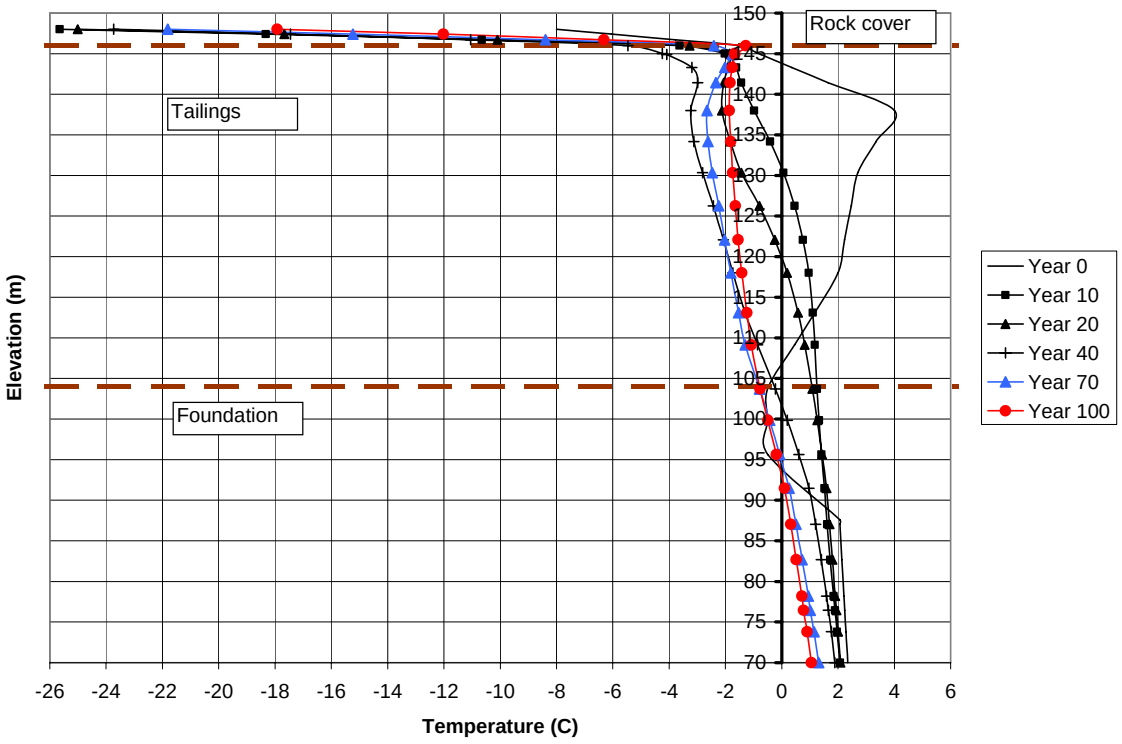

Figure 18 – Evolution of Tailings and Foundation Temperature for Winter (February) Times after the end of Deposition.

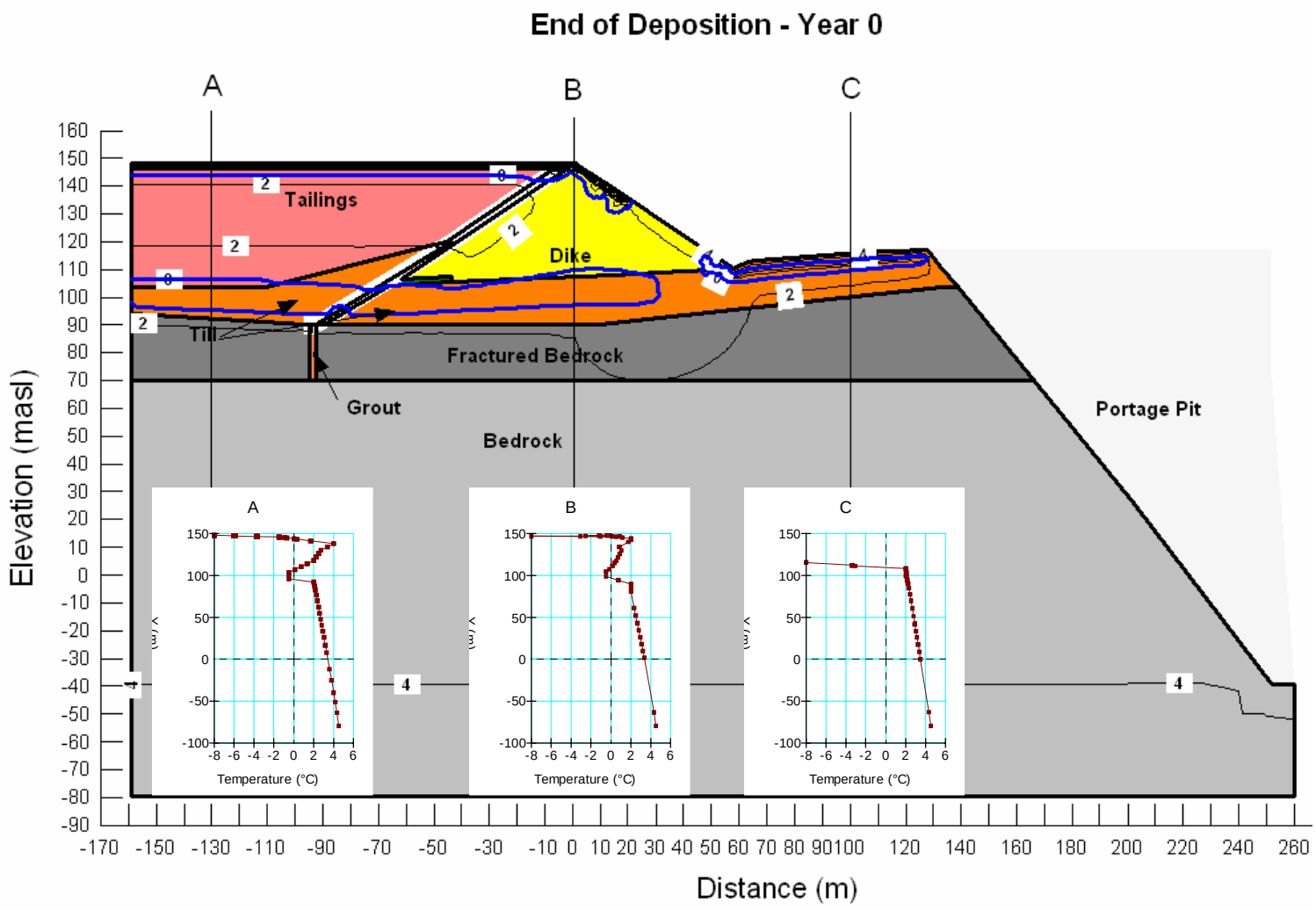

Figure 19 – Temperatures in the TSF at the End of Deposition (February 2013).

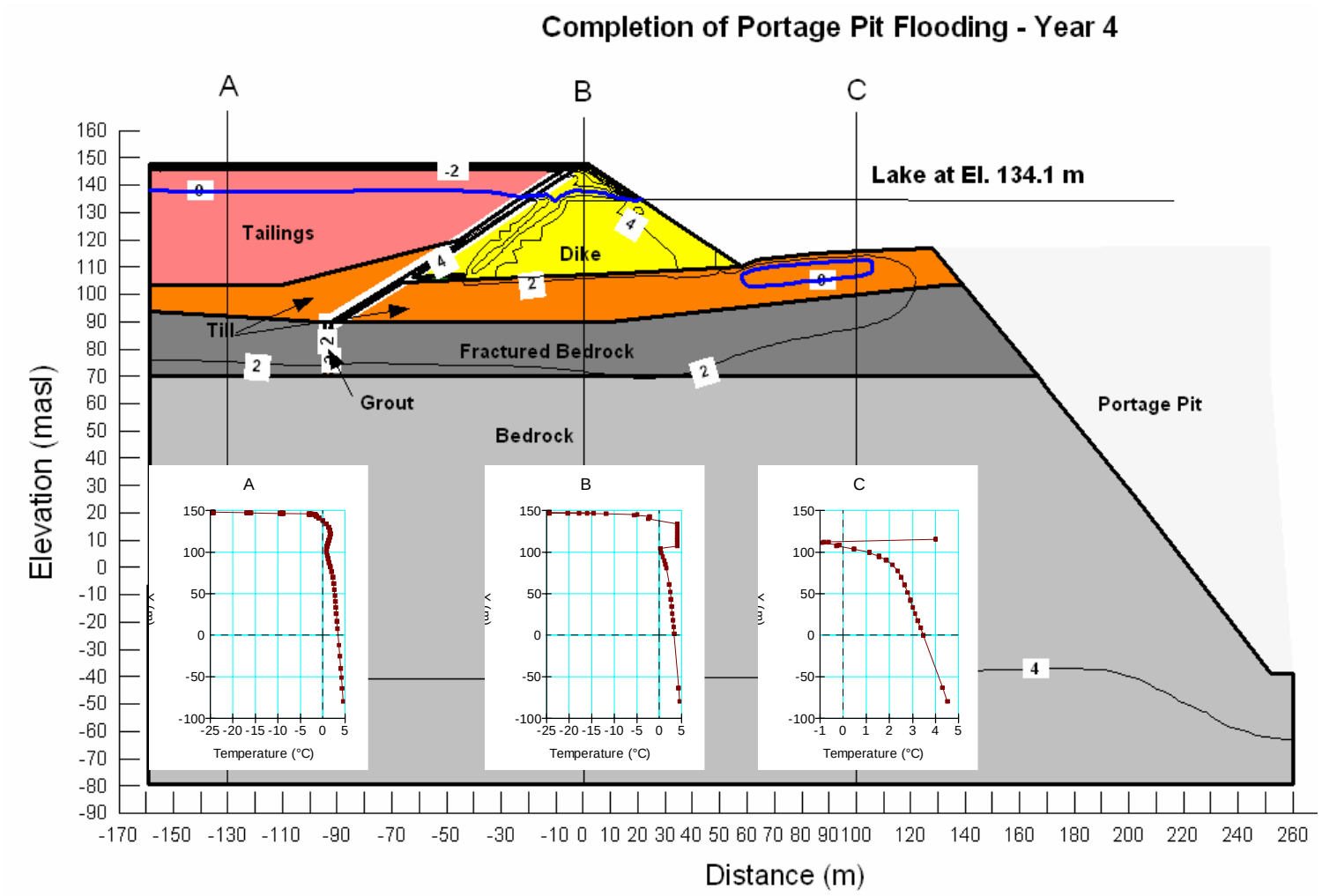

Figure 20 – Temperatures in the TSF after Completion of the Portage Pit Flooding (February 2017).

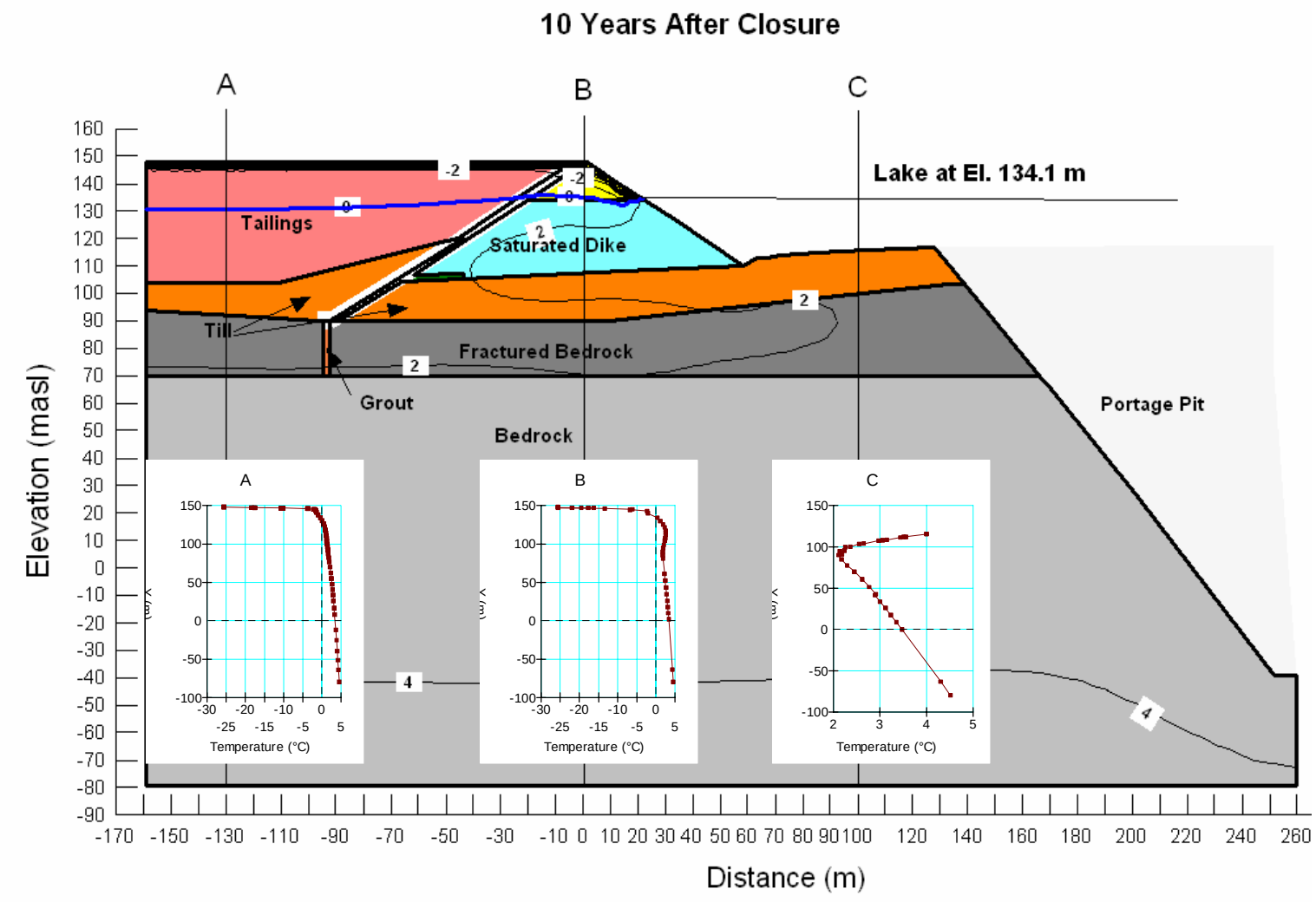

Figure 21 – Temperatures in the TSF 10 Years after Closure (February 2023).

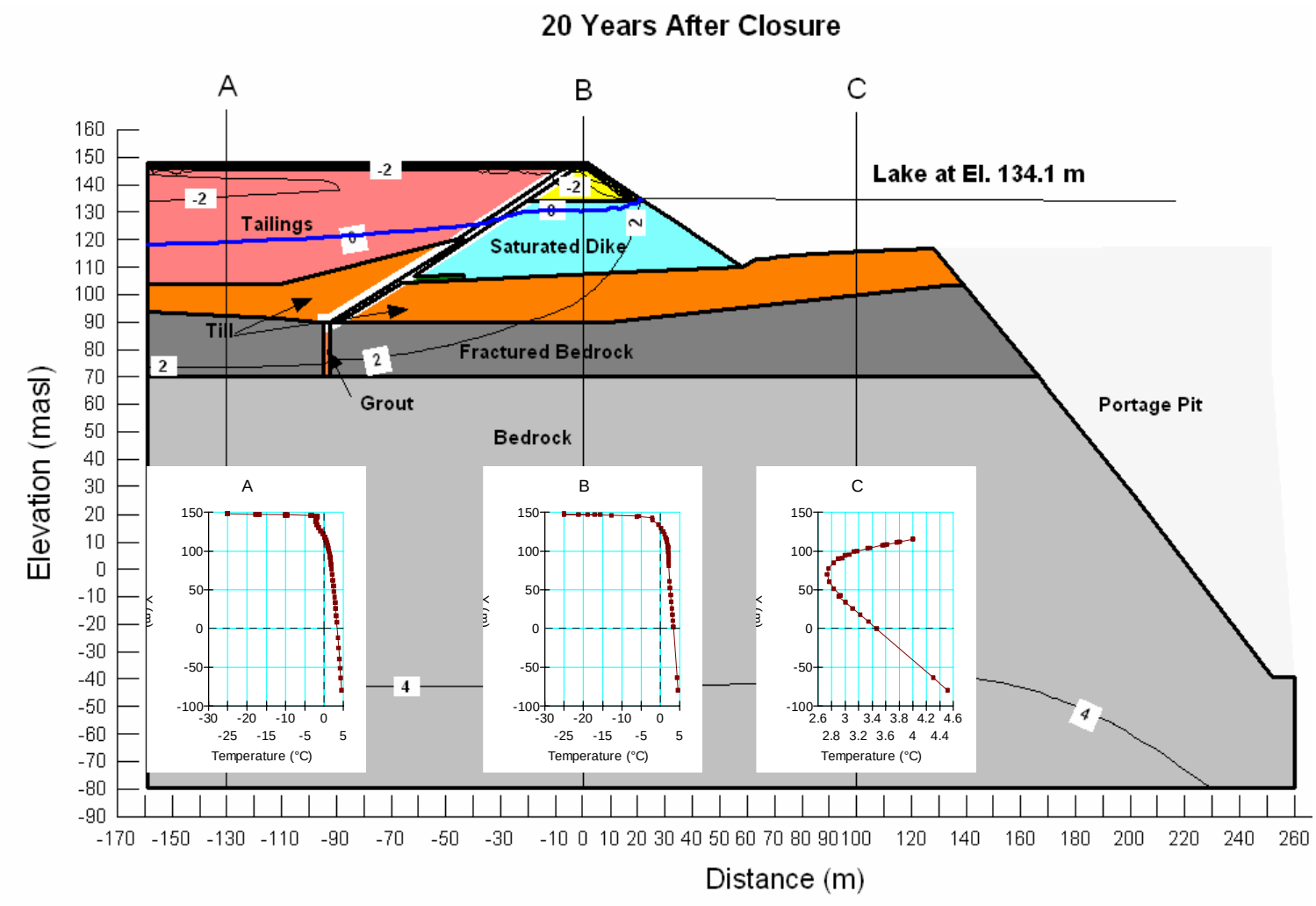

Figure 22 – Temperatures in the TSF 20 Years after Closure (February 2033).

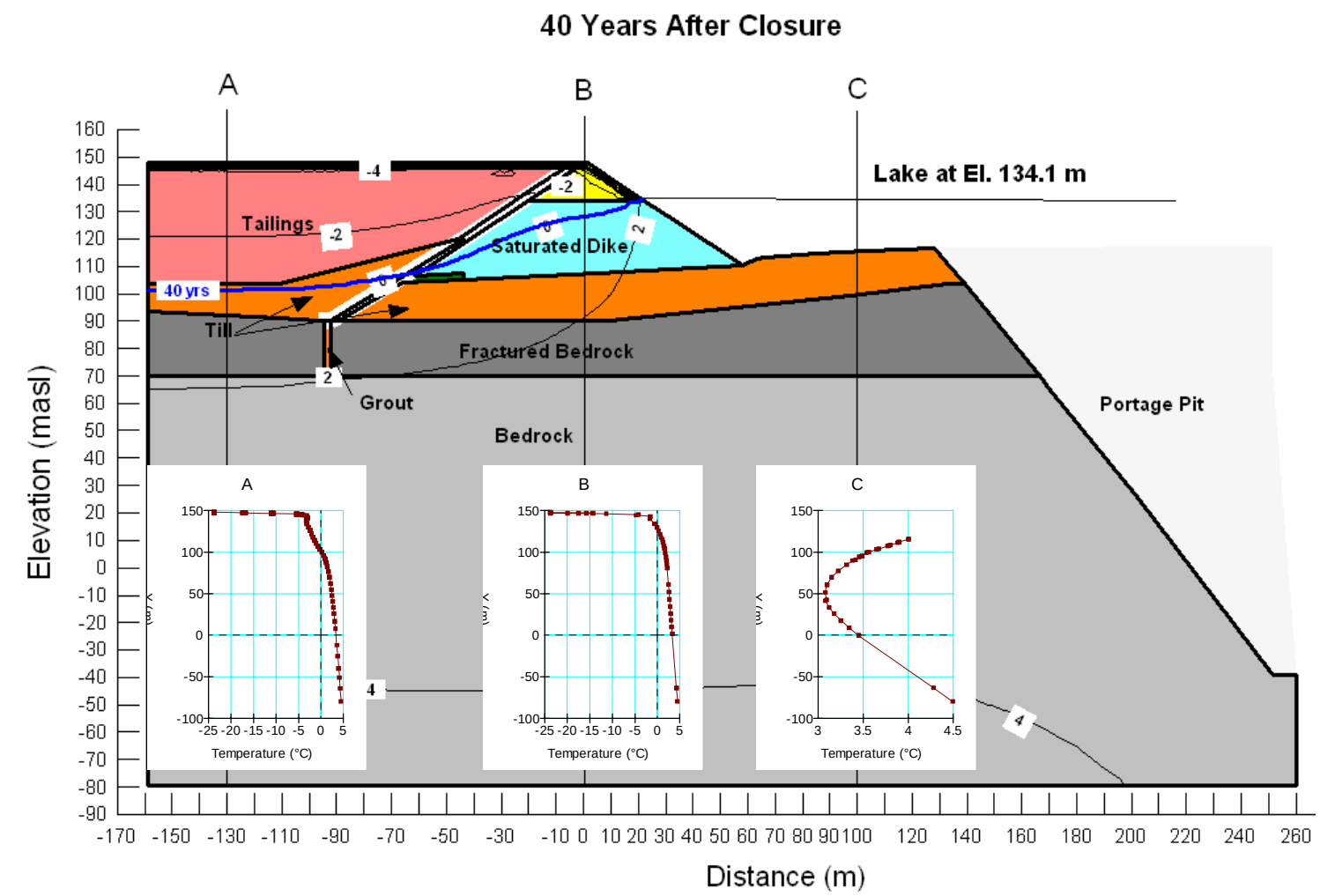

Figure 23 – Temperatures in the TSF 50 Years after Closure (February 2053).

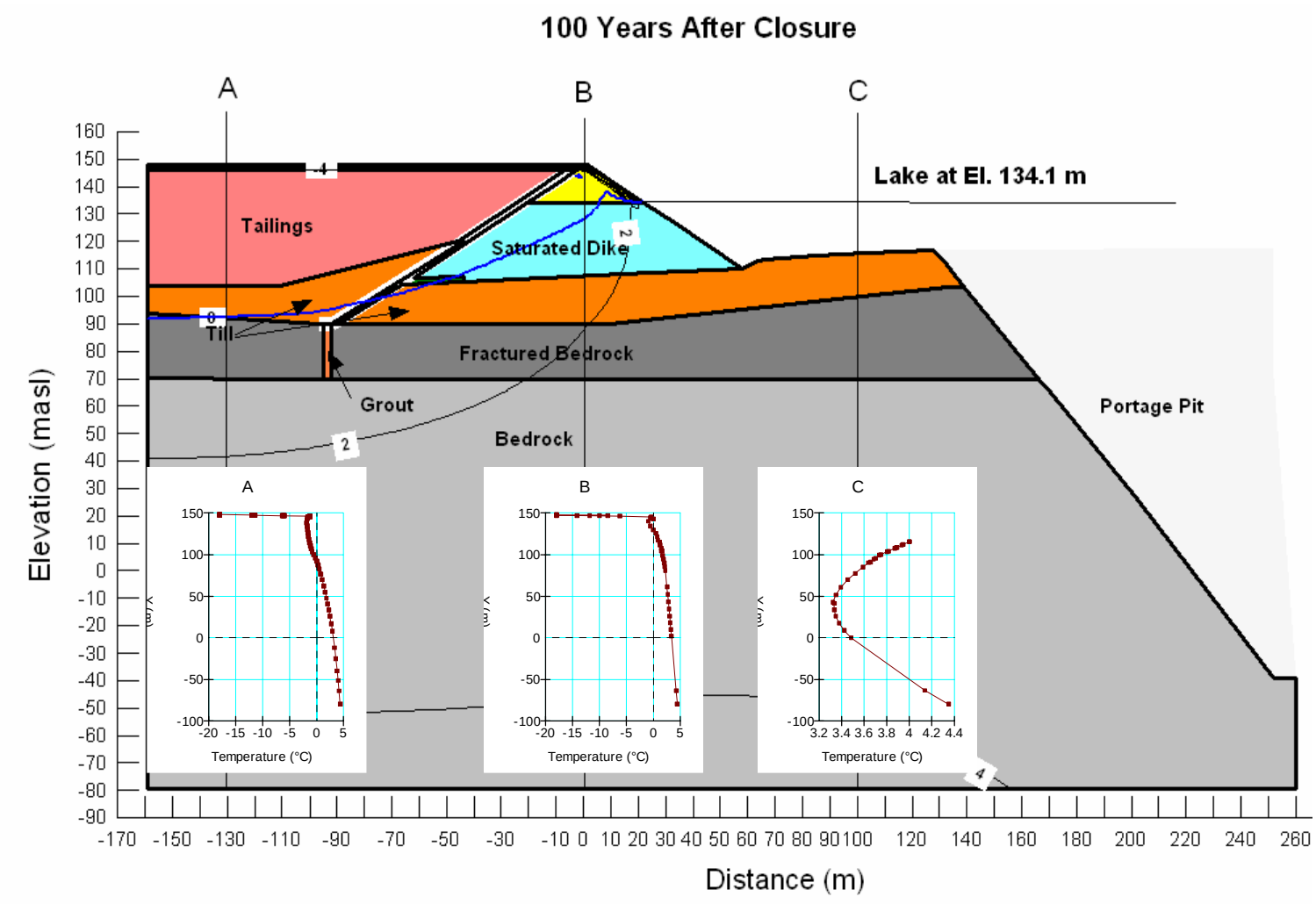

Figure 24 – Temperatures in the TSF 100 Years after Closure (February 2113).

The models indicated that, for the more conservative scenario with most of the tailings unfrozen at the end of deposition, the entire tailings body would be completely frozen within a period of about 40 years after the end of operations. The long term model indicated that the upper portion of the tailings will gradually warm as the mean air temperature increases associated with global warming, but the tailings will remain frozen after a period of 100 years after the mine closure.

The analyses showed that the freezing front will advance into the foundation beneath the tailings in the long term. After approximately 37 years after closure, the freezing front would be at the bottom of the tailings (El. 104 m), deepening to about El. 98 m 50 years after closure, and advancing to about El. 92 m 100 years after closure.

The length of time of about 40 years, required to completely freeze the tailings body is longer than predicted in the first set of analyses carried out early in 2007 (Golder 2007b). This difference in time is mainly associated with flux of water into the permeable dike rockfill during flooding of the Portage Pit, which causes the dike to thaw, requiring additional time to refreeze it. The freezing process of tailings is then affected by the freezing of the dike. In addition, the computed tailings temperature profile at the end of deposition was warmer then previously predicted due to heat carried by infiltrating water.

Nevertheless, the overall pattern of the tailings freeze-back process remained the same as predicted before, with the freezing front gradually deepening with time and advancing into the tailings foundation in the long term. Most of the foundation beneath the Dike will be thawed, controlled by the lake.

Influence of Cryoconcentration in Tailings Temperature

The tailings freezing process may increase the concentration of solutes in the liquid phase due to solute exclusion ahead of the freezing front. Increasing solute concentrations will cause the freezing point of the solution to depress and affect the overall time required to completely freeze the tailings body, as well as affect the amount of liquid in the tailings under sub-zero temperatures. Tailings salinity is also expected to cause the freezing point to depress.

In the field, the solute concentration and tailings salinity will progressively increase associated with the cryoconcentration process, but this increase is not homogeneous and is certain to present spatial variation. The freezing point of locally high solute concentration zones may become lower than the freezing point of surrounding areas, and this will cause liquid high concentration solutions to be trapped within frozen portions. This localized process is not captured in the models.

General sensitivity analyses were carried out to assess average changes in the tailings temperature and water content associated with depressing the freezing point. Figure 25 shows comparison of temperature profiles in the tailings with time computed for freezing points of 0°C and -2°C. Figure 26 shows the computed unfrozen volumetric water contents for both scenarios.

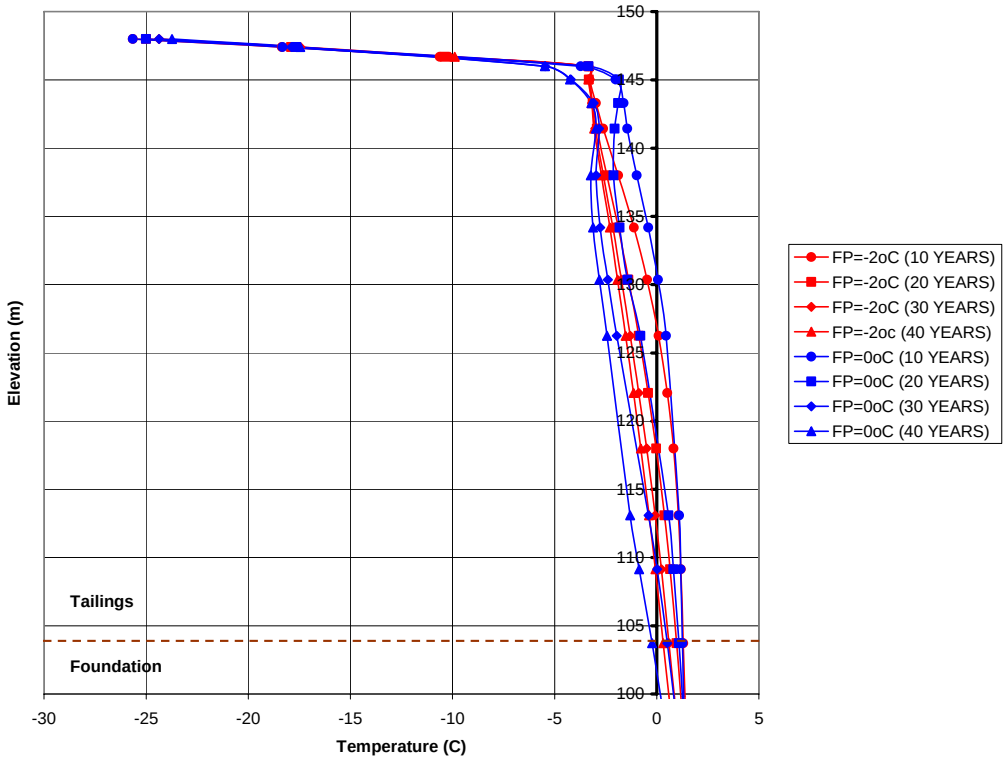

Figure 25 – Comparison of Tailings Temperature Profiles with Time for Depressed Freezing Point.

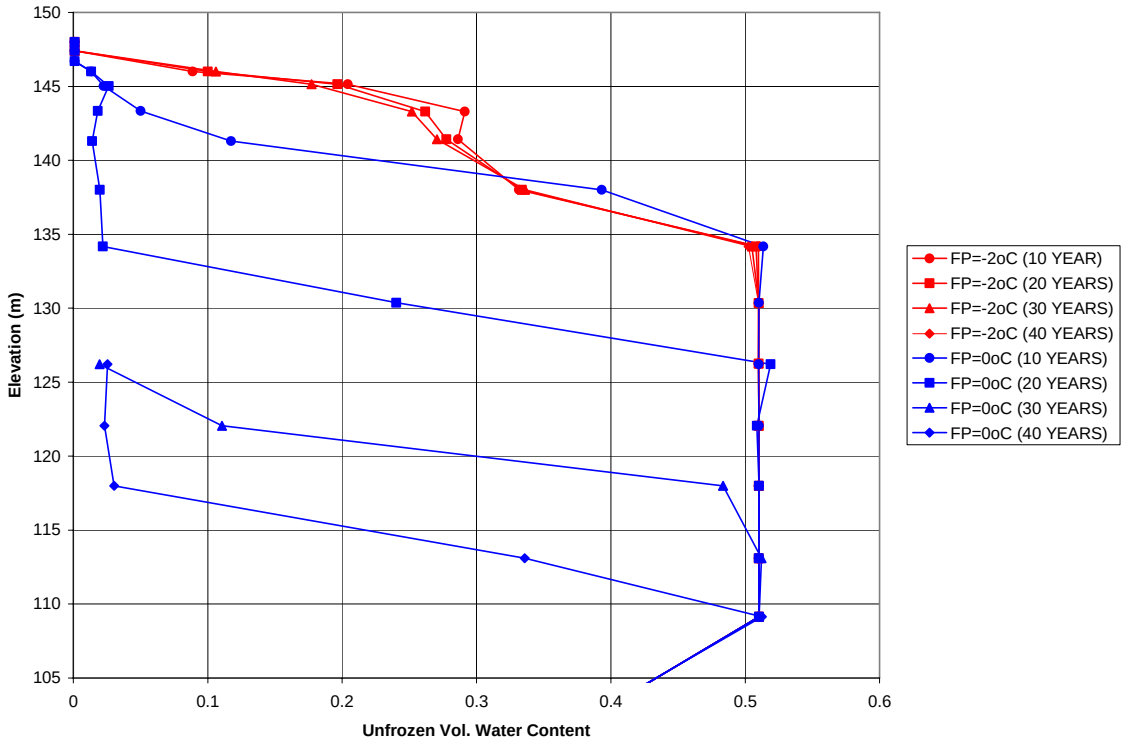

Figure 26 – Comparison of Unfrozen Water Content in the Tailings for Depressed Freezing Point.

As seen in the figures above, the tailings temperature profile at year 10 after closure is colder for the -2°C freezing point than for the 0°C freezing point, but the temperature profiles computed for the 0°C phase change are cooler for years 20 to 40. This happens because temperature typically drops quickly to the freezing point, and then remains at the phase change temperature until all the latent heat is removed. After that, the temperature decreases.

Therefore, if the freezing point depresses to -2°C, initially the temperature will drop faster to -2°C than when a 0°C phase change exists, resulting in cooler temperature profiles. However, for the -2°C phase change the temperature remains at -2°C longer than for the 0°C freezing point scenario, resulting in cooler temperature profiles existing for a 0°C phase change in the long term.

It is important to note that the total unfrozen water content of the tailings for the -2°C freezing point is always higher than for the 0°C phase change scenario. For 0°C phase change, the unfrozen water content progressively reduces with time as the freezing front advances in depth. For the -2°C freezing point, although temperatures are progressively reducing with time, the reduction in volumetric water content is much lower because, in that scenario, water remains in the liquid phase at temperatures of -2°C.

Thus, the general sensitivity analyses indicated that, increasing the concentrations of solute in the tailings will cause water to remain longer at liquid state, and hence sustain water flux for a longer period. This causes the overall time to completely freeze the tailings to increase, but will not prevent the tailings from freezing completely with time.

Temperatures in the Rock Cover

It is planned that the tailings area will be capped with 2 m of non-reactive rock at the end of operations to create an insulation layer between the tailings and the air aimed at keeping the active layer above the tailings. Figure 27 shows variation of the active layer over a period of 100 years. Figure 28 shows the evolution of temperatures at the top and bottom of the rock cover over the same period.

The model indicated that the very low thermal conductivity of the unsaturated rock cover will cause the active zone to remain within the limits of the rock cover in the long term. Global warming will cause temperatures to rise gradually, but the bottom of the cover will remain frozen, thereby preventing the top of tailings from thawing.

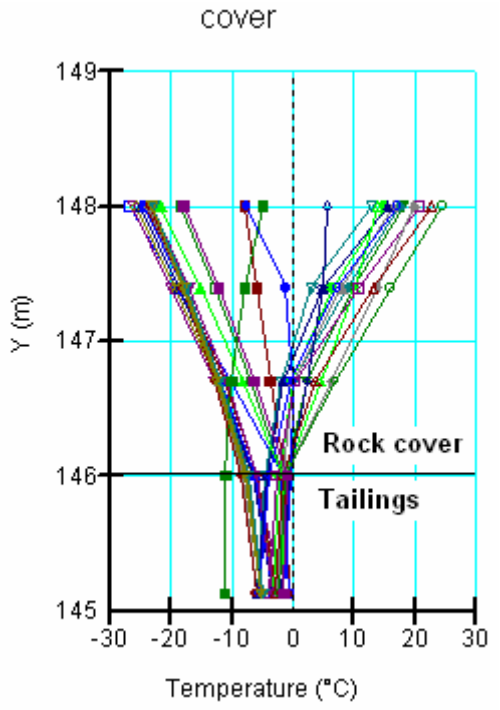

Figure 27 – Variation of the Active Layer within the Rock Cover over a Period of 100 years.

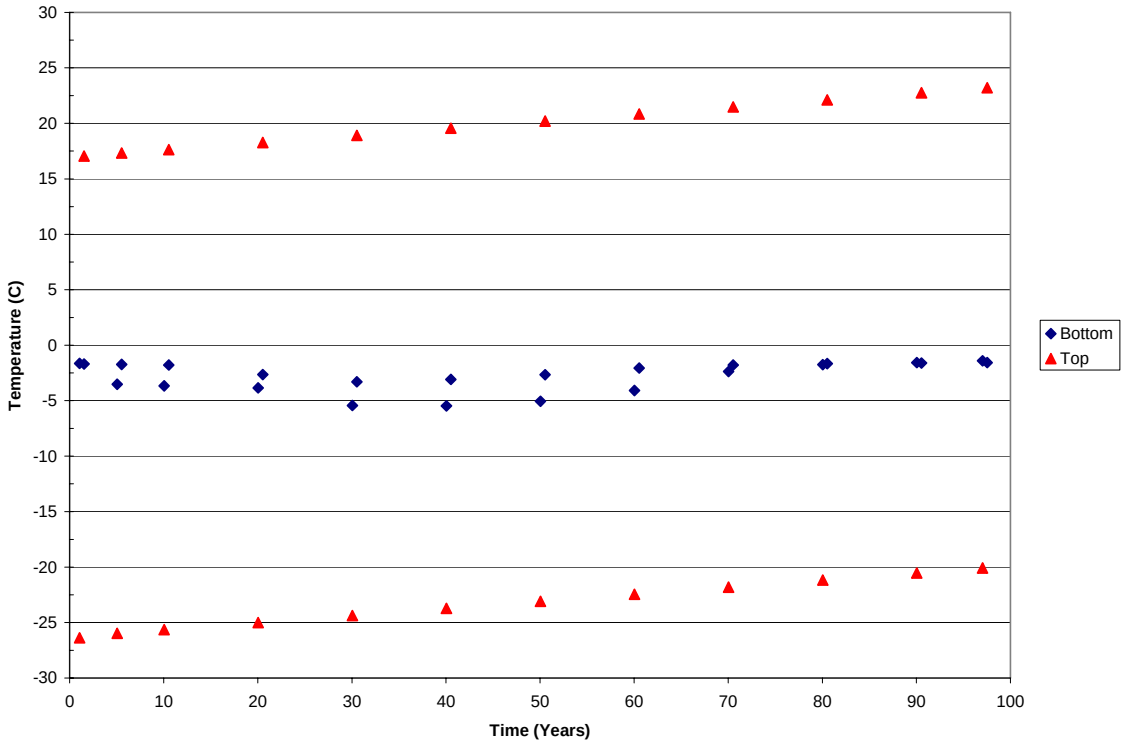

Figure 28 – Evolution of Temperatures at the Top and Bottom of the Rock Cover in the Long Term.

6.2.2 Evolution of Flow Rates

The models indicated that the evolution of flow rates from the tailings to the Portage area after operations will be controlled by two different factors. First, the dynamics of heat exchange between the upper portion of the foundation that is predicted to be frozen after deposition and the thawed tailings and foundation above and below this frozen zone. Second, reduction of the hydraulic gradient between the tailings and the Portage Pit areas.

The 1D model carried out for the tailings deposition phase indicated that at the end of deposition the upper portion of the foundation would be frozen to temperatures of approximately -0.5^{o}C. Under these circumstances, the hydraulic conductivity of the till beneath the tailings will be drastically reduced, and the flow rates will be much lower than the rates that would occur through a thawed foundation. However, the 2D TSF model showed that further heat exchange will cause the upper foundation to thaw, increasing its hydraulic conductivity and causing the flow rate to rise.

The flow rates will also be controlled by the existing hydraulic gradient between the tailings and the Portage Pit areas. Once deposition ceases, the tailings will start to drain down, gradually reducing the water level in the tailings. On the other hand, the level of the Portage Lake will steadily rise to the final elevation of 134.1 m during an assumed period of 4 years. The combination of lowering water table in the tailings and increasing lake level will cause the hydraulic head difference between the two areas to reduce from about 70 m at the end of operations to zero after the lake reaches its final elevation and hydrostatic equilibrium is attained. When the water level in the tailings equals the lake level, hydrostatic equilibrium will exist and the flux of water from the tailings area into the lake will nearly cease.

Figure 29 shows the evolution of flow rates through the bottom of the tailings during flooding of the Portage Pit and after the lake reaches its maximum elevation of 134.1 m.

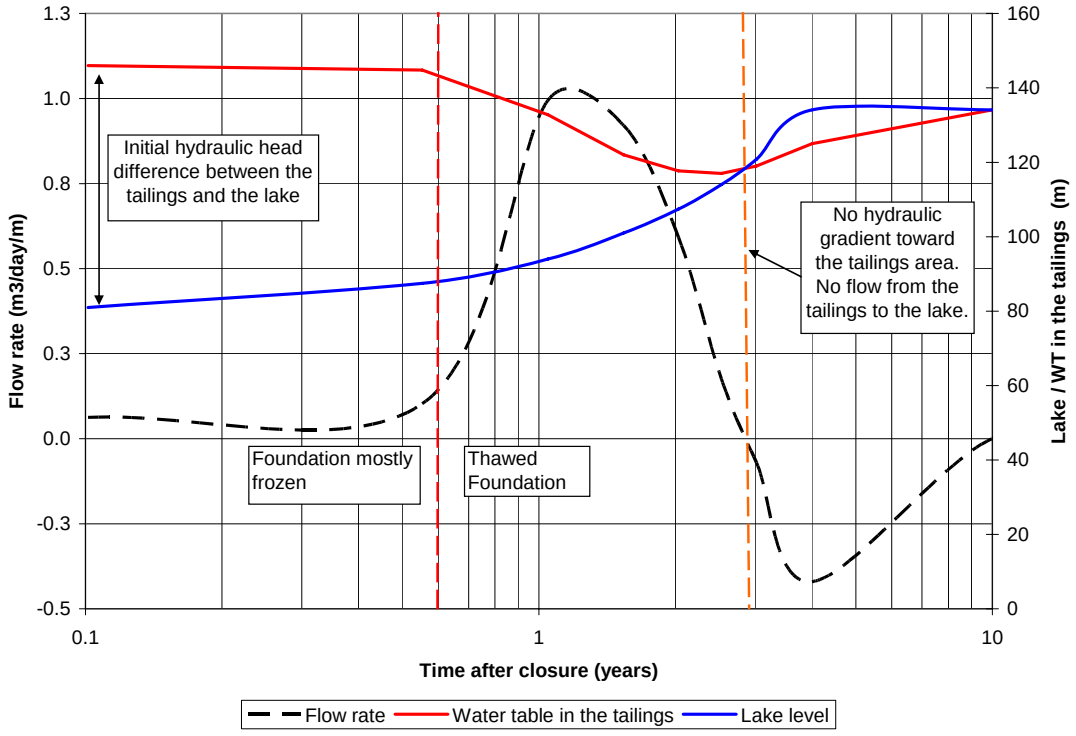

Figure 29 – Evolution of Flow Rates Through the Foundation with time and Hydraulic Gradient between the Tailings and the Lake.

As seen in Figure 29, initially the flow rate is mainly controlled by the heat exchange mechanism. The frozen foundation restricts water flow through the bottom of tailings during operations and shortly after the deposition phase is complete, but continuous heat

exchange will cause the upper foundation to thaw, thereby markedly increasing its hydraulic conductivity and causing the flow rate to have a sharp rise. Then, the flow rate will gradually reduce again due to reduction in the hydraulic gradient between the tailings and the lake.

The models indicated that the lake level would equal the water level in the tailings at elevation of approximately 119 m. After that, the lake rises faster than the rise of water table in the tailings, and the hydraulic gradient reverts toward the tailings area, preventing water flux from the tailings to the lake. Once the lake reaches its final elevation of 134.1 m, the water level in the tailings will continue to rise to the same elevation of the lake. At that point, no significant hydraulic gradient will exist between the two areas and water flow will cease. Figure 30 shows the water table location during flooding of the Portage Pit.

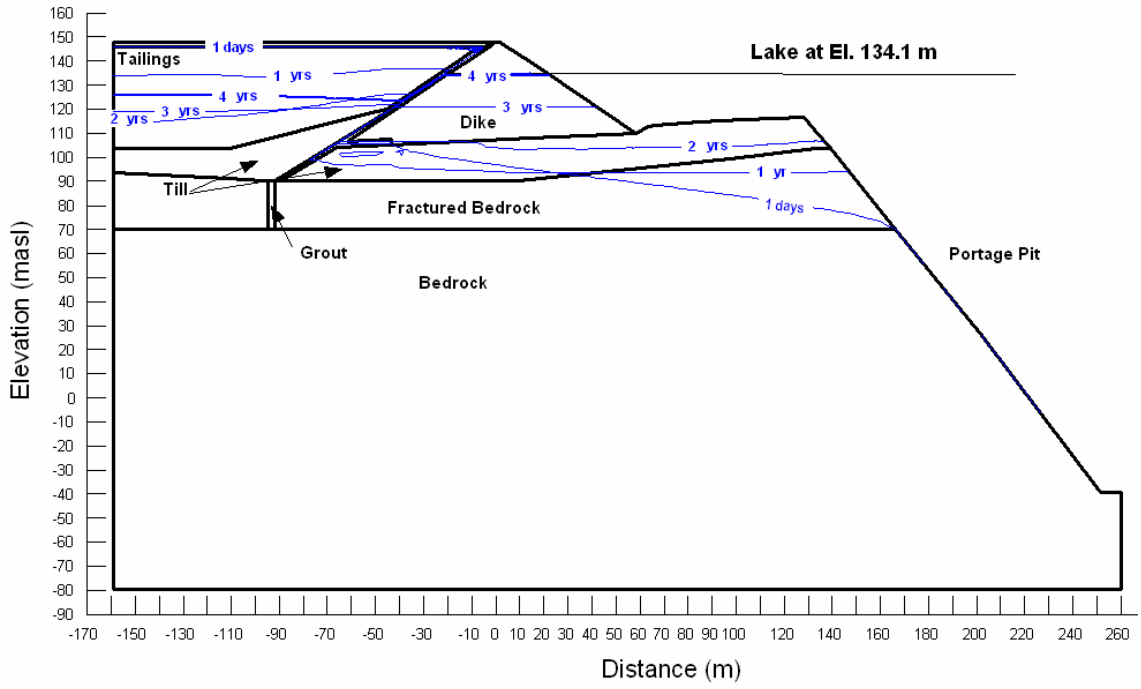

Figure 30 – Variation of the Water Table Location in the Tailings Storage Facility during Flooding of the Portage Pit.

Flow Rates through the Portage Fault

The pattern of evolution of flow rates through the fault is similar to that computed for the TSF away from the fault, but the flow rates through the fault are greater. In addition, the model indicated that the portion of the tailings that lies above the fault zone will tend to drain down faster, and the water table in the tailings will lower near the fault zone, reducing the local hydraulic gradient between the tailings and the Portage Pit.

The model computed peak flow rate is about 3.7 m^3/day/m associated with the thawed foundation. Flow rate then reduces quickly, controlled by the reduction in the hydraulic gradient. Figure 31 shows the evolution of flow rates through the fault zone after the end of deposition.

If a thawed foundation develops during operations, the maximum flow rate computed through the fault zone with a hydraulic head of 70 m between the tailings area and the Portage Pit was 6.1 m^3/day/m, or about 3.5 times the maximum flow rate computed for areas away from the fault (1.7 m^3/day/m). It is however important to differentiate the contribution of each component to the total flow that would occur through the Central Dike, considering its design basal length of 570 m. Table 6 presents the total maximum flow through the Central Dike combining the flow through the fault and through areas away from the fault for thawed and frozen foundation scenarios.

TABLE 6: Maximum Flow Rates Predicted through the Central Dike

Foundation condition	Tailings WT El. at peak flow (m)	Groundwater at Portage Pit (m)	Flow through Fault (x 5 m width) m^3/day	Flow away from the fault (x 565 m length) m^3/day	Combined Flow Rate (m^3/Day)
Thawed	146 m (Deposition)	75 m (Deposition)	31	961	992
Frozen during deposition	128 m (After closure)	94 m (Pit flooding)	19	532	551

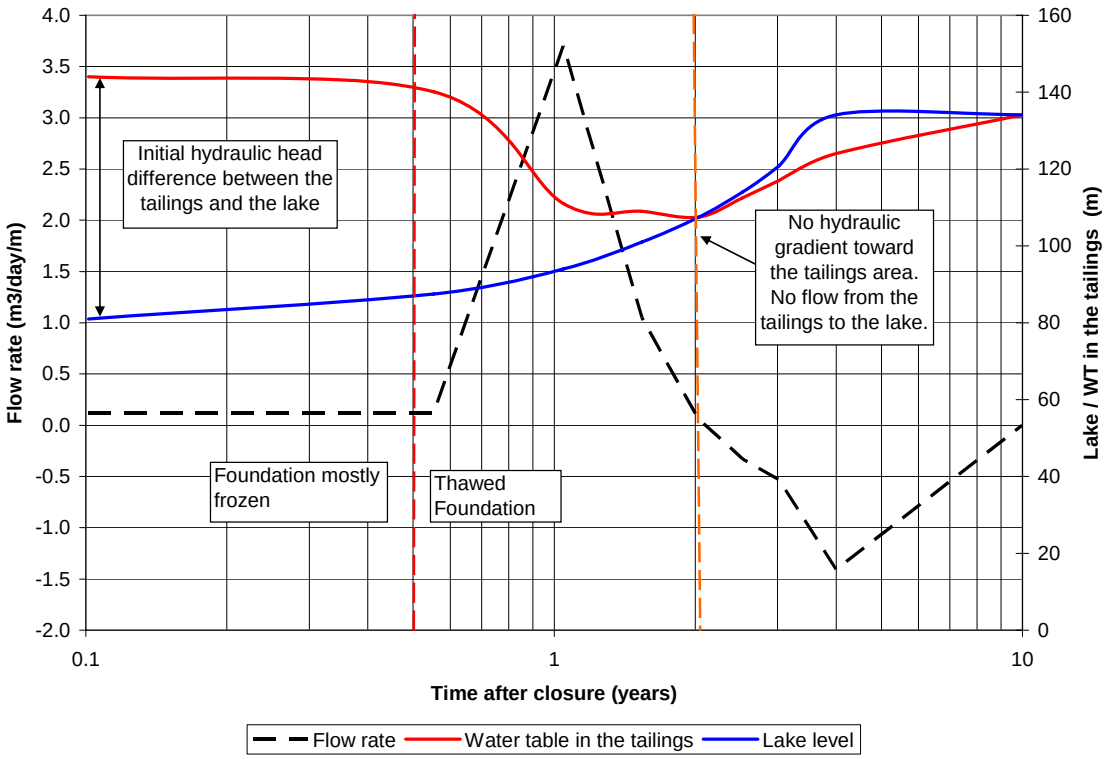

Figure 31 – Evolution of Flow Rates through the Portage Fault with Time and Hydraulic Gradient Between the Tailings and the Lake.

Assessment of Transport of Contaminants

Due to the relatively high hydraulic conductivity of the till in the upper foundation, the advection process will mainly govern the transport of contaminants in the area, with minor influence of diffusion. As a result, the pattern of transport of contaminants broadly follows the evolution of flow rates.

Transport of contaminants will be restricted during operations due to the low permeability of the frozen foundation, but the loads increase after the foundation thaws and flow rates increase. However, the hydraulic gradient between the tailings and the Portage Pit areas decreases as a result of the rising lake level and lowering water table in the tailings. This causes the flow rates, and consequently the contaminant loads, to reduce to near zero about 3.5 years after the end of operations. Once the lake level becomes higher than the water table in the tailings, the hydraulic gradient reverses to the tailings area and drives water back into the tailings until the water table in the tailings equals the lake level.

Figure 32 shows the evolution of the normalized contaminants loads with time after the end of operations. Figure 33 shows the converted evolution of Cu and Cyanide loads based on the estimated tailings water quality (Golder 2007c).

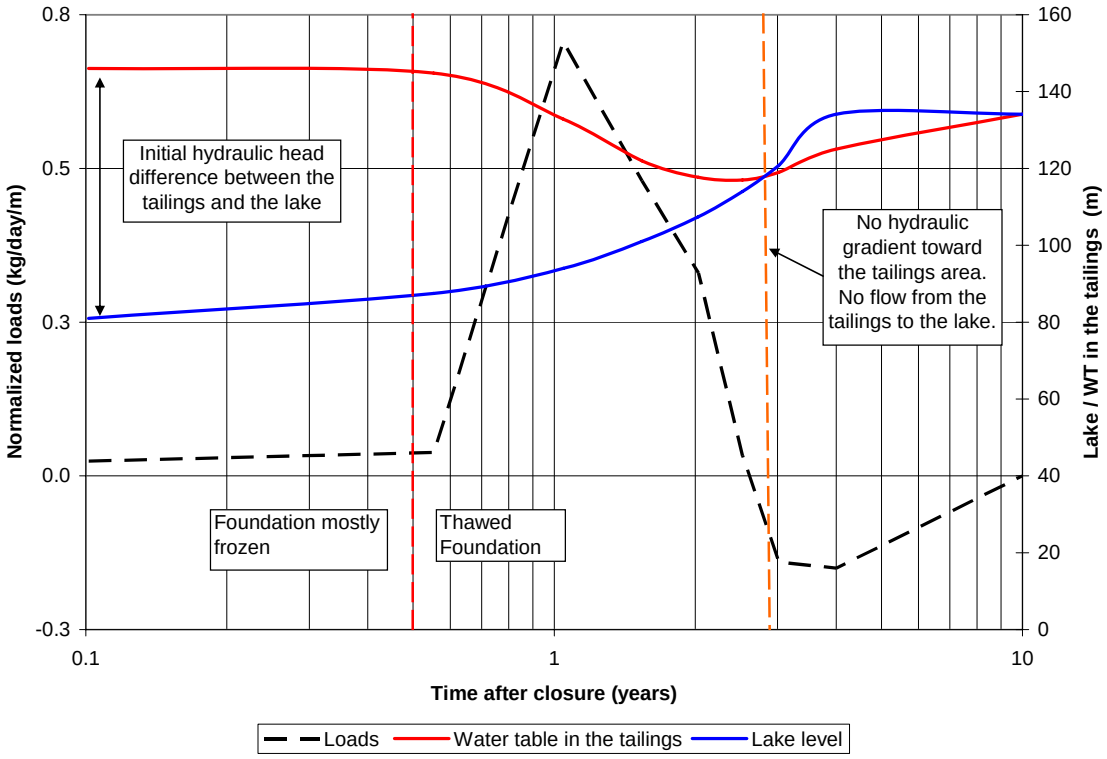

Figure 32 – Evolution of Contaminant Loads from the Bottom of the Tailings after the Mine Closure.

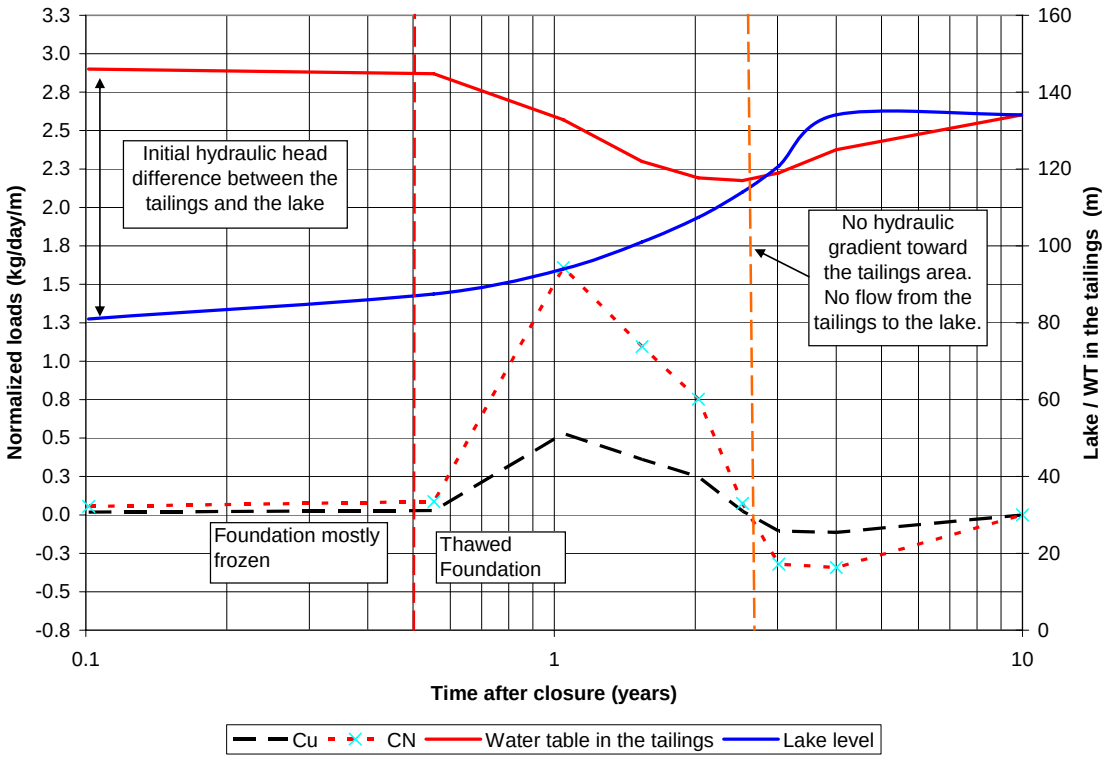

Figure 33 – Evolution of Copper and Cyanide Loads from the Bottom of the Tailings after the Mine Closure.

The models indicated that the contaminants that started to be released from the bottom of the tailings after the foundation thaws will not arrive to the area of the Portage Pit due to reduction of flow velocities associated with a lower hydraulic gradient. Figures 34 to 36 show the normalized concentration of contaminants in the foundation with time.

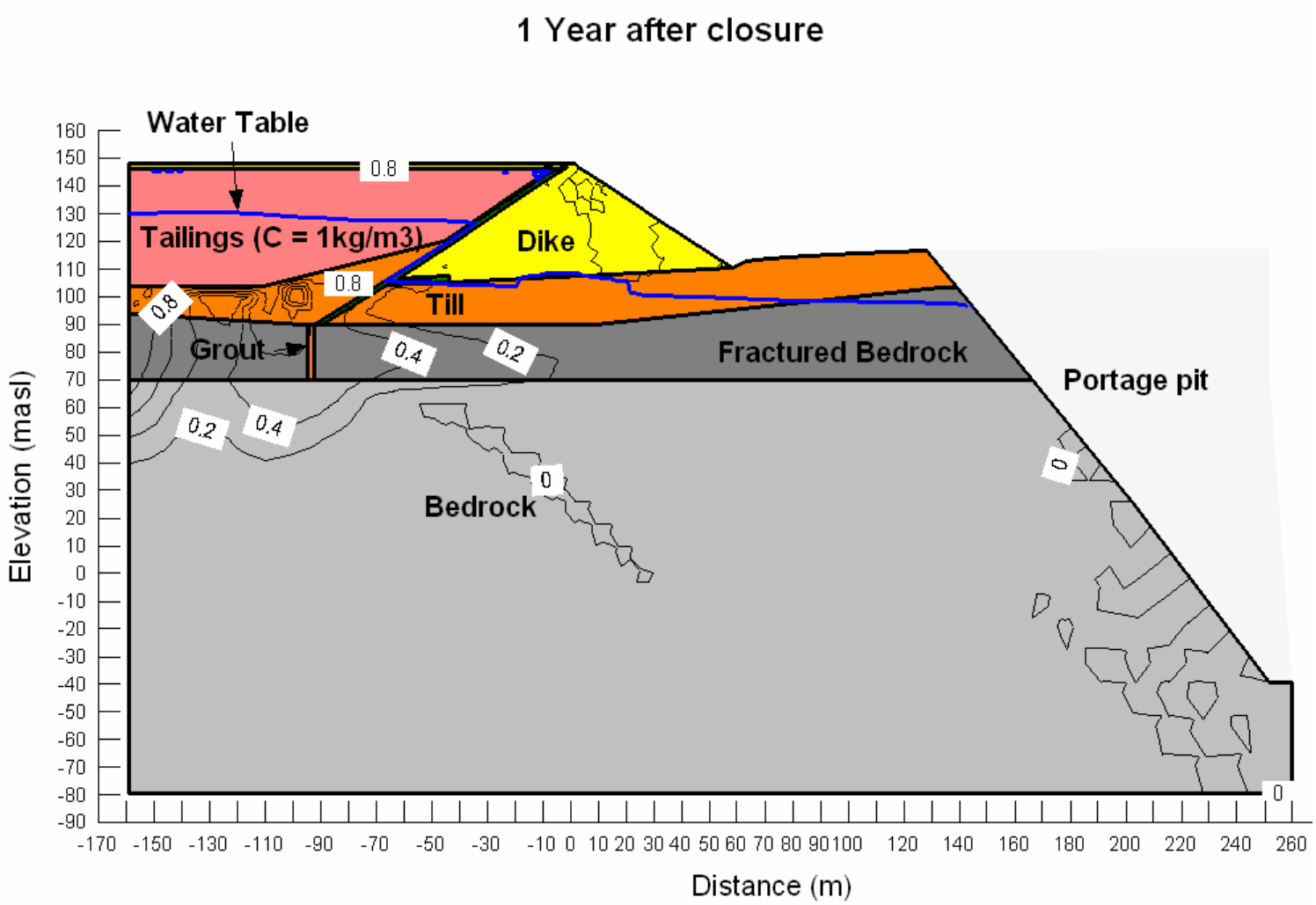

Figure 34 – Concentration of Contaminants in the Foundation 1 year after the Mine Closure

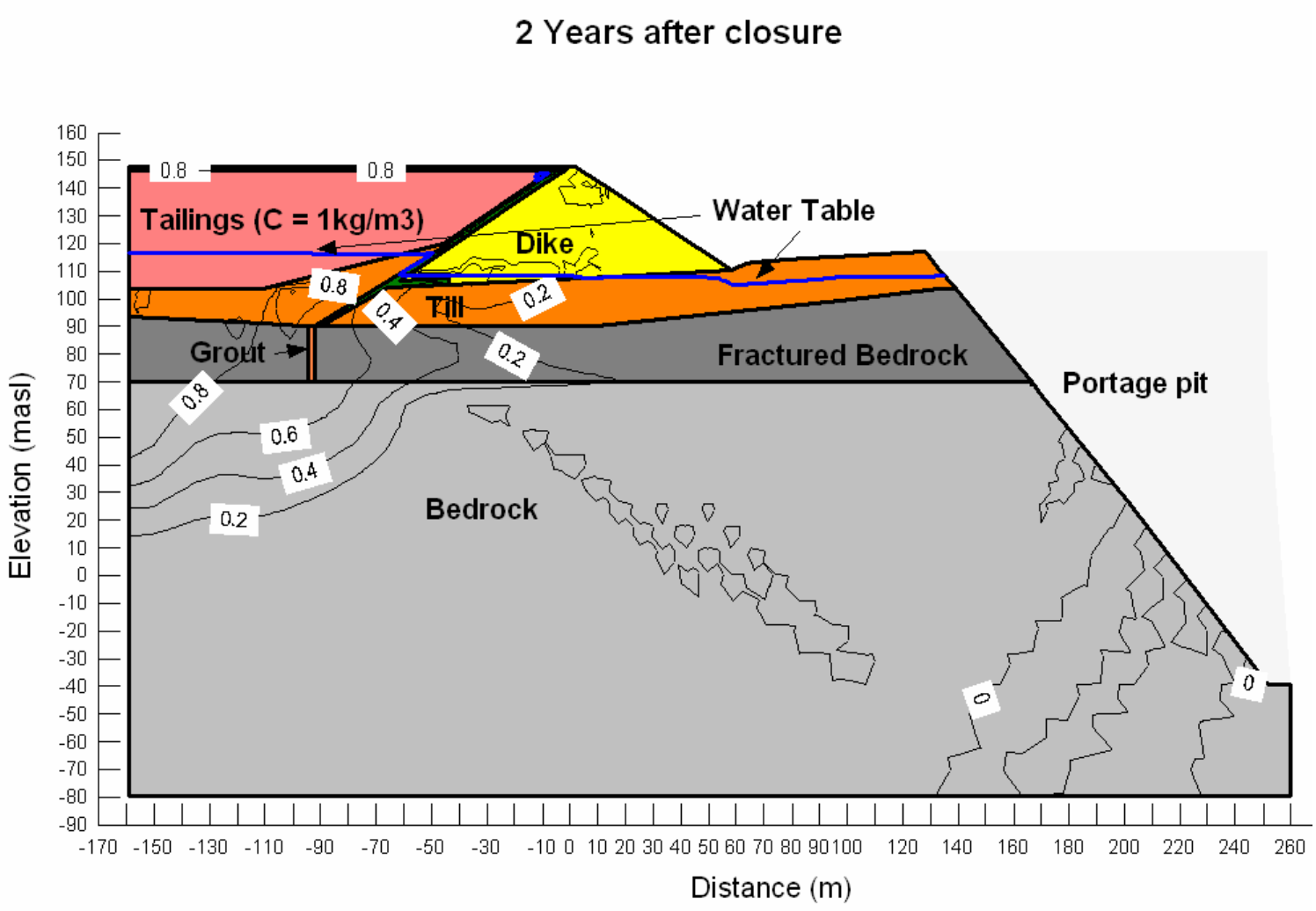

Figure 35 – Concentration of Contaminants in the Foundation 2 years after the Mine Closure

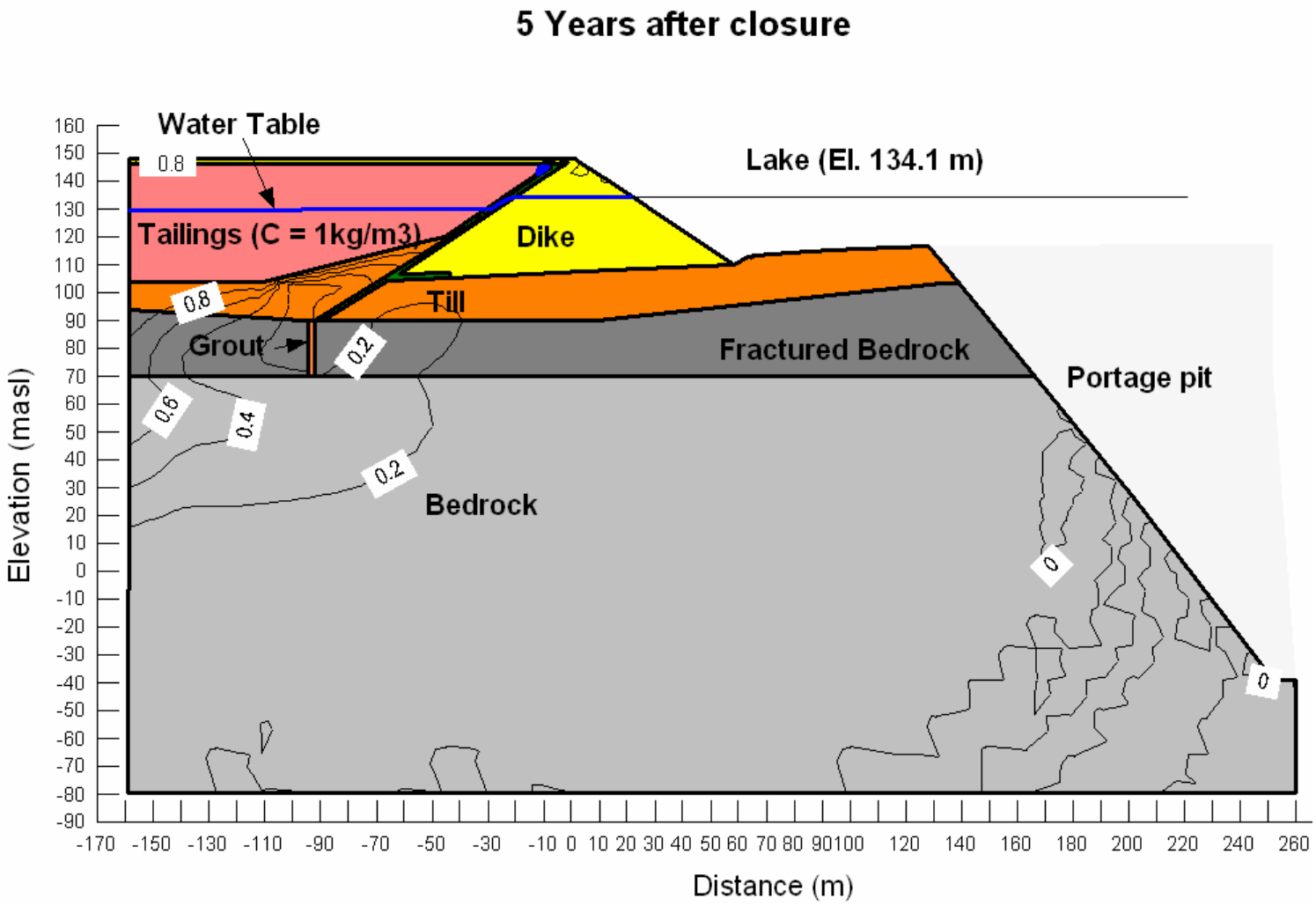

Figure 36 – Concentration of Contaminants in the foundation 5 years after the Mine Closure

6.2.3 Sensitivity to Thawed Foundation During Deposition

The concentration of contaminants described above were computed based on reduced flow rates after deposition associated with an upper frozen foundation with low hydraulic conductivity. A sensitivity analysis was performed to assess what the concentrations would be if the foundation is thawed during deposition and after closure. Under this scenario, transport of contaminants would start together with deposition, and contaminants would reach the Portage Pit before the end of operations. Figure 37 shows the evolution of contaminant loads during and after deposition at three different locations: bottom of the tailings, across the grouting curtain and, near the edge of the Portage Pit. The three locations are shown in Figure 38 that also shows the normalized concentrations of contaminants in the foundation after completion of the Portage Pit flooding.

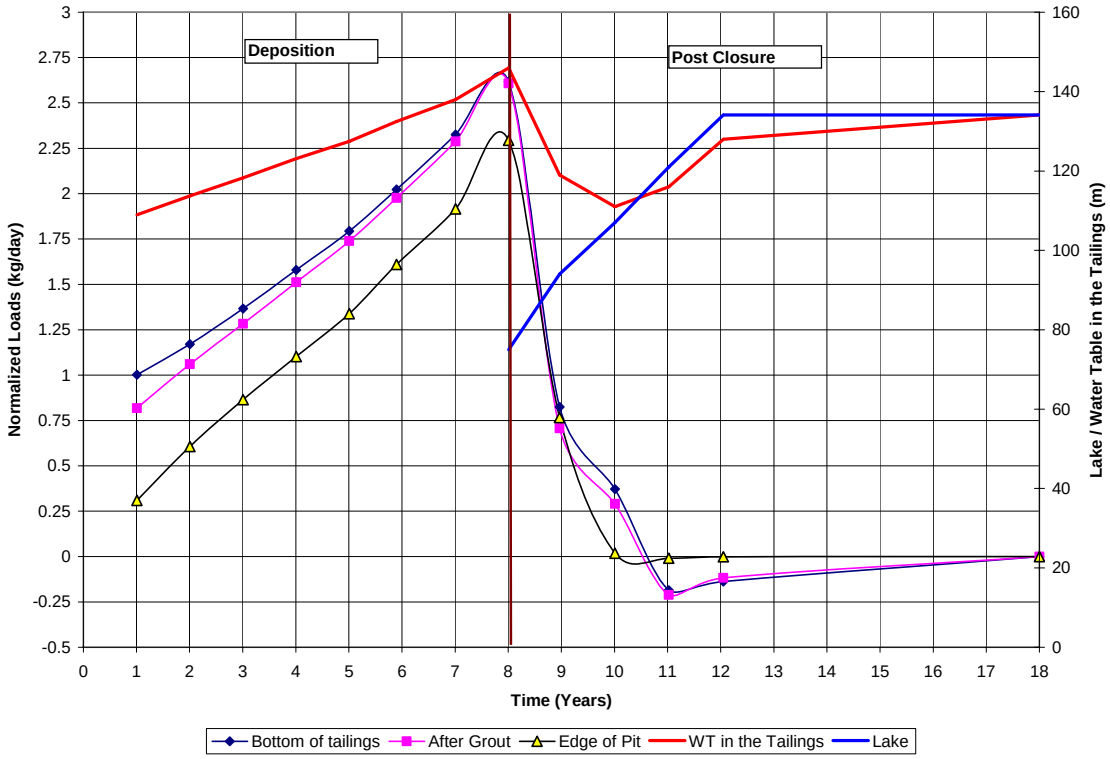

Figure 37 – Evolution of Contaminants Loads during Deposition and after Closure Considering a Thawed Foundation.

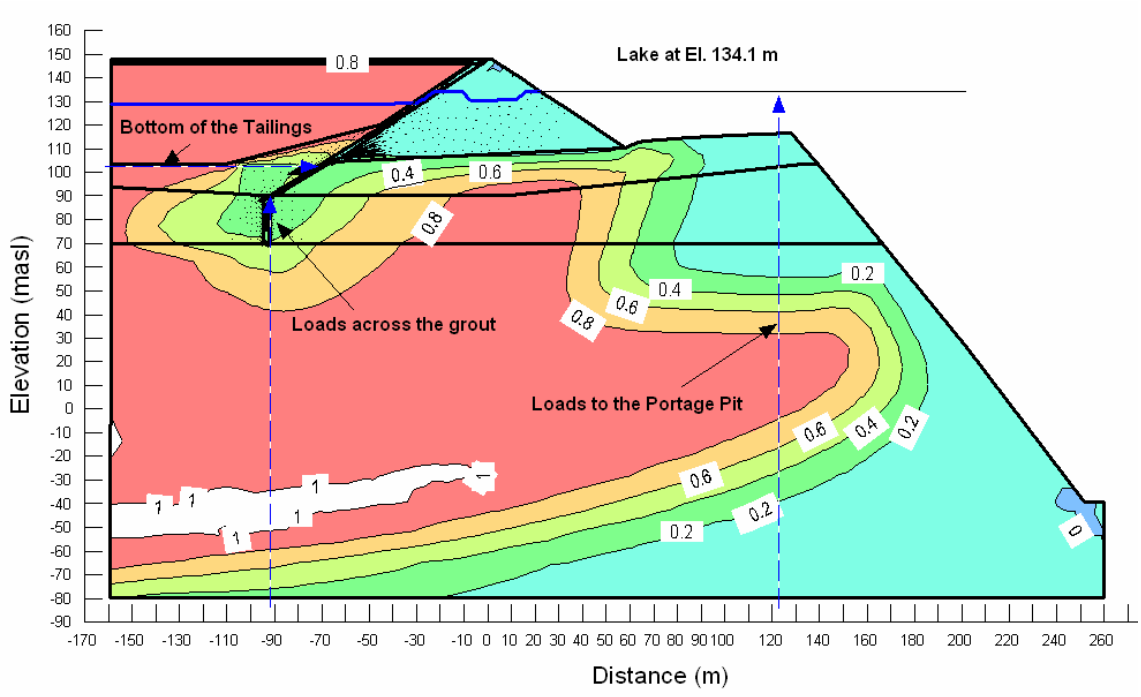

Figure 38 – Normalized Concentration of Contaminants in the TSF Foundation after Completion of the Portage Pit Flooding Considering a Thawed Foundation.

The sensitivity analysis showed that, with a thawed foundation, contaminants would be transported during operations, and the loads would progressively increase as the hydraulic gradient between the tailings and the Portage Pit increases. The model also indicated that contaminants would reach the Portage Pit area during operations.

At the end of operations, the tailings would drain down faster than for the frozen foundation case, associated with the higher hydraulic conductivity of the thawed foundation. This will cause the hydraulic gradient between the tailings area and the Portage Pit to reduce faster as well, thereby reducing the contaminant loads. Once the lake level becomes higher than the water table in the tailings, the hydraulic gradient would reverse toward the tailings area, and clean water would flow from the lake into the foundation, causing the overall concentration of contaminants to reduce by dilution. When the water table in the tailings equals the lake level, the hydraulic gradient will be reduced to near zero, and no water flux and contaminant loads will occur.

Therefore, for a thawed foundation scenario, while the groundwater beneath the tailings area would still present contaminants after completion of the Portage Pit flooding, the transport of contaminants into the lake would cease associated initially with the near-zero hydraulic gradient, and later with the progressive freezing of the tailings.

7.0 CONCLUSIONS

Thermal analyses were carried out early in 2007 to evaluate the evolution of the tailings freeze-back process at the Meadowbank Gold Project site. Encapsulation of tailings within the continuous permafrost zone is the main strategy planned to isolate the tailings area from adjacent lakes, thereby preventing migration of contaminants toward the lake. The 2007 study indicated that the tailings would freeze completely with time, and therefore the chosen strategy was considered efficient.

Upon comments made by Natural Resources Canada (NRCan), additional coupled thermal and seepage analyses were carried out to evaluate the impact of flowing water in the temperature regimes of the Tailings Storage Facility during operations and post closure phase. Furthermore, contaminant transport analyses were semi-coupled with the thermal/seepage analyses to evaluate the process of transport of contaminants in the area.

In order to evaluate the evolution of tailings temperatures during deposition, a sequential 1D model was developed based on the tailings depositional plan. For the conservative conditions assumed, the models indicated that at the end of operations most of the tailings body would be thawed, with the existence of a frozen zone at the bottom of the tailings that partially extends to the upper foundation. The computed temperature profile was then transferred to a 2D seep/thermal/contaminant model aimed to assess the thermal regime in the TSF.

The 2-D TSF model used a typical section of the Central Dike, with tailings deposited in the upstream area, and the Portage Pit located near the downstream face of the dike. Upon the mine closure, the model considered flooding of the Portage Pit during a period of 4 years, with the lake reaching its final elevation of 134.1 m.

The model indicated that the upper part of the dike would be frozen at end of operations, but this zone will then thaw affected by the rising lake level during flooding of the Portage Pit. The long-term analysis indicated that the lake will then govern the temperatures downstream of the Central Dike, while the tailings will control the patterns of temperatures in the upstream portion of the Central Dike.

The analyses showed that the tailings will gradually freeze with time, being completely frozen within a period of about 40 years after closure. The freezing front will then extend to about 20 m into the foundation, keeping both the tailings and foundation frozen in the long-term. The overall length of time required to completely freeze the tailings is longer than predicted in the previous study done in 2007. The main reasons for this change are the thawing of the dike during flooding of the Portage Pit, and water flux through the tailings.

The models also indicated that global warming will progressively increase the tailings temperature, but will not cause the tailings to thaw during the 100 year period analyzed.

In terms of flow rates, the models indicated that water flux will be restricted during operations associated with an upper frozen foundation with low hydraulic conductivity. After the end of operations, this upper frozen zone will thaw upon continuous heat exchange with the warmer tailings above and thawed foundation beneath the frozen zone. Once the foundation thaws, the flow rates are expected to increase related to increasing hydraulic conductivities. However, the flow rates will then reduce due to reduction of the hydraulic gradient between the tailings and the Portage Pit areas. The hydraulic gradient will reduce associated with the progressive increase of the lake level during flooding of the Portage Pit, and lowering of the water table in the tailings after completion of deposition. Once the lake reaches its final elevation of 134.1 m, and the water table in the tailings equals this level, the hydraulic gradient will be reduced to near zero, and flux from the tailings area into the lake will essentially cease.

Additional analysis indicated that the flow rates through the Portage Fault will be about three times greater than the flow rates away from the fault zone. However, the impact of this greater flow rate in the total predicted flow rates through the Central Dike will be minor because the Portage Fault is inferred to be only 5 m wide, while the total dike length is about 570 m.

Contaminant analyses were conducted semi-coupled with the thermal/seepage analyses. The flow velocities computed in the thermal/seepage analyses were used to compute the advection of contaminants through the foundation toward the Portage Pit area. The first scenario considered that contaminants will not be transported during operations due to flux restrictions associated with the frozen foundation. Contaminant transport would then start after closure, upon thawing of the upper foundation, but the models indicated that the contaminants would not reach the area of the Portage Pit as flow velocities decrease progressively together with reduction of the hydraulic gradient between the tailings and the Portage Pit areas.

A sensitivity analysis was conducted considering a thawed foundation during operations and post closure. The results showed that contaminant transport would start during the deposition phase, and that the contaminants would reach the area of the Portage Pit. However, upon the mine closure and flooding of the Portage Pit, pit water will infiltrate the foundation and reduce the contaminant concentrations through dilution. Furthermore, the transport of contaminants will be reduced as the hydraulic gradient between the tailings and the Portage Pit areas approaches zero.

Contaminant transport will therefore be reduced initially due to the reduction of the hydraulic gradient and flow velocities, and later the tailings freeze-back process will prevent movement of contaminant from the tailings area to the lake.

GOLDER ASSOCIATES LTD.

ORIGINAL SIGNED BY

Fernando Junqueira, Ph.D, P.Eng. (BC)
Senior Geotechnical Engineer

ORIGINAL SIGNED AND SEALED BY

Terry Eldridge, P.Eng. (NWT, NT)
Principal

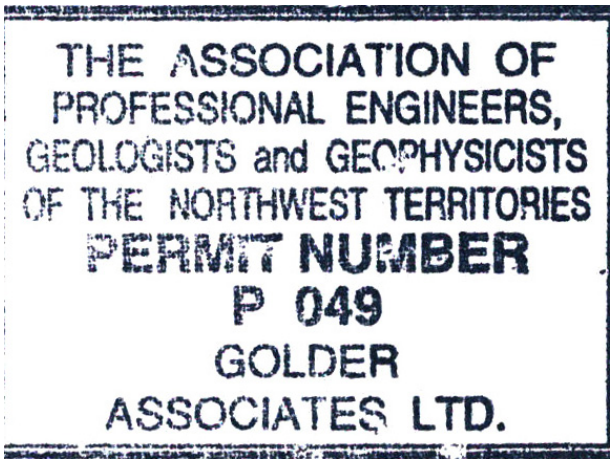

FJ/DRW/TLE/lw/rs
O:\Final\2007\1413\07-1413-0074\Doc 722 0801_08 Rpt Coupled Thermal Seepage and Containment Modeling-Tailings Facility Ver 0.doc

8.0 REFERENCES

Anderson, D., Tice, A., and McKim, H., 1973. The Unfrozen Water Content and the Apparent Heat Capacity in Frozen Soils. Proceedings, 2nd International permafrost conference, Yakutsk, pp289-295

Fetter C. W. (2001). Applied Hydrogeology 4th ed. p. 400. Prentice Hall Inc. ISBN:
0-13-088-239-9 pg.

GEOSLOPE Ltd (2004). Thermal Modeling with TEMP/W. An Engineering Methodology. TEMPW User Manual. Calgary, May 2004.

Golder Associates Ltd. (2007a). Technical Memorandum – Testing and Monitoring of Faults. February 2007.

Golder Associates Ltd. (2007b). Final Report – Detailed Design of Central Dike - Meadowbank Project. March 2007.

Golder Associates Ltd. (2007c). Report on Water Quality Predictions – Meadowbank Gold Project. August 2007.

Intergovernmental Panel on Climate Change (IPCC) (2007). Climate Change 2007: The Physical Science Basis.

Johansen, Ø. 1975. Thermal Conductivity of Soils. Ph.D. Diss., Norwegian Technical Univ., Trondheim; also, U.S. Army Cold Reg. Res. Eng. Lab. Transl. 637, July 1977.

Johnston, G.H., Ladanyi. B., Morgenstem, N.R., and Penner, E. (1981). Engineering Characteristic of Frozen and Thawing Soils. Permafrost Engineering Design and Construction. Edited by John Wiley & Sons.

MEND (1998). Acid Mine Drainage Behaviour in Low Temperature Regimes. Thermal Properties of Tailings. MEND Project 1.62.2. July 1998.

Nidal H. et all (2000) , Soil Thermal Conductivity. Effects of Density, Moisture, Salt Concentration, and Organic Matter Soil Science Society of America Journal 64:1285-1290 (2000)

Nixon, J. F. (1991) Discrete Ice Lens Theory for Frost Heave in Soils, Canadian Geotechnical Journal, Volume 28, 843-859.